



January 2017

## Geophysical Analysis Of The Paleogeothermal Gradient And Heat Flow In The Williston Basin, ND

Daniel Burke Brunson

[How does access to this work benefit you? Let us know!](#)

Follow this and additional works at: <https://commons.und.edu/theses>

---

### Recommended Citation

Brunson, Daniel Burke, "Geophysical Analysis Of The Paleogeothermal Gradient And Heat Flow In The Williston Basin, ND" (2017). *Theses and Dissertations*. 2179.  
<https://commons.und.edu/theses/2179>

This Thesis is brought to you for free and open access by the Theses, Dissertations, and Senior Projects at UND Scholarly Commons. It has been accepted for inclusion in Theses and Dissertations by an authorized administrator of UND Scholarly Commons. For more information, please contact [und.commons@library.und.edu](mailto:und.commons@library.und.edu).

GEOPHYSICAL ANALYSIS OF THE PALEOGEOTHERMAL GRADIENT AND HEAT  
FLOW IN THE WILLISTON BASIN, ND

by

Daniel Burke Brunson  
Bachelor of Science, The University of Alabama, 2006  
Bachelor of Science in Geology, The University of Alabama, 2013

A Thesis

Submitted to the Graduate Faculty

of the

University of North Dakota

in partial fulfillment of the requirements

for the degree of

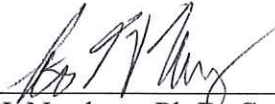
Master of Science

Grand Forks, North Dakota  
December  
2017

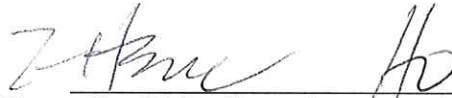
This thesis, submitted by Daniel Burke Brunson in partial fulfillment of the requirements for the Degree of Master of Science from the University of North Dakota, has been read by the Faculty Advisory Committee under whom the work has been done and is hereby approved.



William D. Gosnold, Ph.D, Chairperson

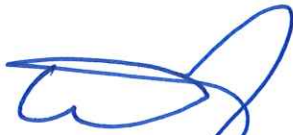


Stephan H. Nordeng, Ph.D, Committee Member



I-Hsuan Ho, Ph.D, Committee Member

This thesis is being submitted by the appointed advisory committee as having met all of the requirements of the School of Graduate Studies at the University of North Dakota and is hereby approved.



Grant McGimpsey  
Dean of the School of Graduate Studies



Date

## PERMISSION

Title            Geophysical Analysis of the Paleogeothermal Gradient and Heat Flow in the  
                    Williston Basin, ND

Department    Geology

Degree         Master of Science

In presenting this thesis in partial fulfillment of the requirements for a graduate degree from the University of North Dakota, I agree that the library of this University shall make it freely available for inspection. I further agree that permission for extensive copying for scholarly purposes may be granted by the professor who supervised my thesis work or, in his absence, by the Chairperson of the department or the dean of the School of Graduate Studies. It is understood that any copying or publication or other use of this thesis or part thereof for financial gain shall not be allowed without my written permission. It is also understood that due recognition shall be given to me and to the University of North Dakota in any scholarly use which may be made of any material in my thesis.

Daniel Burke Brunson  
December 7, 2017

## TABLE OF CONTENTS

LIST OF FIGURES .....	vi
LIST OF TABLES.....	viii
LIST OF ACRONYMS .....	ix
ACKNOWLEDGEMENTS .....	xi
ABSTRACT .....	xii
CHAPTER	
I.    BACKGROUND .....	1
II.   PROJECT INTRODUCTION.....	3
Overview .....	3
Statement of Hypothesis.....	4
Study Setting.....	4
Thermal Energy Generation and Flow in the Earth’s Crust .....	9
Thermal Conduction.....	10
Steady State Thermal Conduction.....	11
Factors of Elevated Geothermal Gradients and Heat Flow .....	12
III.  METHODS.....	13
Overview .....	13
Thermostратigraphy.....	13
Steady State Conductive Heat Flow Modeling.....	17

IV.	RESULTS .....	21
	Overview .....	21
	Thermostratigraphy .....	21
	Steady State Conductive Heat Flow Modeling.....	28
V.	DISCUSSION.....	34
	Thermostratigraphy.....	34
	Steady State Conductive Heat Flow Modeling.....	35
IV.	CONCLUSIONS .....	37
	APPENDICES .....	38
	Appendix A. Thermostratigraphy Datasets .....	39
	Appendix B. Heat Flow Profiles Datasets .....	48
	REFERENCES .....	49

## LIST OF FIGURES

Figure	Page
1. Location and outline of the Williston Basin showing major basement structures.....	5
2. Location and outline of the study area within western North Dakota.....	15
3. Locations of wells used in the present study .....	16
4. Mean heat flow values occurring within the area of study.....	17
5. Computer screen capture of an ARC model simulation in progress.....	19
6. Plot of computed temperatures of NDGS #25 .....	22
7. Plot of computed temperatures of NDGS #527 .....	22
8. Plot of computed temperatures of NDGS #607 .....	23
9. Plot of computed temperatures of NDGS #2010 .....	23
10. Plot of computed temperatures of NDGS #2615 .....	24
11. Plot of computed temperatures of NDGS #6464 .....	24
12. Plot of computed temperatures of NDGS #6616 .....	25
13. Plot of computed temperatures of NDGS #7020 .....	25
14. Plot of computed temperatures of NDGS #7783 .....	26
15. Plot of computed temperatures of all well used in this study .....	27

16.	Results of heat flow simulation model run for 35 my duration .....	29
17.	Plot of simulated thermal event evolution taking place in heat flow models.....	30
18.	Plot of surface heat flow change over geologic time in the 35 my heat flow model.....	31
19.	Plot of surface heat flow change over geologic time in the 65 my heat flow model.....	32



## LIST OF TABLES

Table	Page
1. Ages and thermal conductivities of Williston Basin formations .....	8
2. TSTRAT calculations for NDGS well #25.....	39
3. TSTRAT calculations for NDGS well #527.....	40
4. TSTRAT calculations for NDGS well #607.....	41
5. TSTRAT calculations for NDGS well #2010.....	42
6. TSTRAT calculations for NDGS well #2615.....	43
7. TSTRAT calculations for NDGS well #6464.....	44
8. TSTRAT calculations for NDGS well #6616.....	45
9. TSTRAT calculations for NDGS well #7020.....	46
10. TSTRAT calculations for NDGS well #7783.....	47
11. Surface heat flow profile calculations for 35 my heat flow model.....	48
12. Surface heat flow profile calculations for 65 my heat flow model.....	48

## LIST OF ACRONYMS, UNITS, EQUATIONS, AND SYMBOLS

Symbol	Name	Units
<b>A</b>	Radioactive Heat Production or HPU	$\mu\text{W m}^{-3}$
$^{\circ}\text{C}$	Celsius	$^{\circ}\text{C}$
$\frac{dT}{dz}$	Geothermal Gradient	$^{\circ}\text{C m}^{-1}$
<b>HC</b>	Hydrocarbon	(not applicable)
<b>K</b>	Kelvins	K
<b>km</b>	Kilometers	km
$\lambda$	Thermal Conductivity	$\text{W m}^{-1} \text{K}^{-1}$
<b>MI</b>	(Hydrocarbon) Maturity Indices ( $R_o$ , $T_{\text{max}}$ )	(not applicable)
<b>m</b>	Meters	m
<b>mW</b>	Milliwatt	mW
<b>mW m<sup>-2</sup></b>	Milliwatts per Meter Squared	$\text{mW m}^{-2}$
<b>q</b>	(Crustal) Heat Flow	$\text{mW m}^{-2}$
<b>Q</b>	Thermal Energy Content	Joules
<b>R<sub>o</sub></b>	Vitrinite Reflectance	% $R_o$
<b>T</b>	Temperature	K or $^{\circ}\text{C}$
<b>TOC</b>	Weight % of Total Organic Carbon	(not applicable)
<b>T<sub>0</sub></b>	Surface Temperature	K or $^{\circ}\text{C}$
<b>T<sub>max</sub></b>	ROCK-EVAL	mg HC/g rock
<b>T-z plot</b>	Temperature vs. Depth Plot	$^{\circ}\text{C}$ vs. m
<b>TSTRAT</b>	Thermostratigraphy	$^{\circ}\text{C m}^{-1}$
<b>v</b>	Volume	$\text{m}^3$

<b>z</b>	Vertical Depth	m
<b>ND</b>	North Dakota	(Not applicable)
<b>NDGS</b>	North Dakota Geological Survey	(Not applicable)
<b>WB</b>	Williston Basin	(Not applicable)
$q = \frac{dT}{dz} \lambda$	Fourier's Law of Heat Conduction	mW m <sup>-2</sup>
$Q = q_0 + Ab$	Relationship between Heat Flow and Production	mW m <sup>-2</sup>
$T_z = \sum_{i=1}^n \frac{qz_i}{\lambda_i}$	TSTRAT Equation	°C

## ACKNOWLEDGEMENTS

The author wishes to thank Dr. William Gosnold, Dr. I-Hsuan Ho, and Dr. Stephan Nordeng for their willingness to participate in my thesis work, particularly for their understanding. Special thanks are due to Dr. William D. Gosnold for his help and guidance during this work.

The author also wishes to express gratitude to the State of North Dakota and the North Dakota Industrial Commission (NDIC) Oil & Gas Section for granting access to the historical and present data generated by the oil & gas industry well drilling operations present within the state.

Most of all, the author would like to thank his parents for their unyielding love and support every day.

I humbly stand on the shoulders of STEM giants who have come before and gave rise to the ease with which scientific experimentation can be conducted at present....

## **ABSTRACT**

Past researchers have suggested that elevated heat flow once existed in the Williston Basin during the Eocene Epoch or younger time frame, based on petroleum maturity indices data. Further, they have argued that those attempting to computationally model the region have incorrectly assumed constant heat flow through time. The present work attempts to address the different positions taken by updating geophysical modeling evidence concerning heat flow in the Williston Basin in which paleogeothermal conditions are variable over geologic time. After conducting the investigation, present research demonstrates that elevated heat flow may have existed in the Williston Basin in the geologic past but did not necessarily have to occur during or after the time period suggested. Furthermore, variable radioactivity in the crystalline basement rock demonstrated by the present models can explain the enhanced thermal maturity described by past researchers. Only more detailed study will eventually lead the scientific community to a more precise explanation of the cause and time constraints of such paleogeothermal conditions.

## **CHAPTER I**

### **BACKGROUND**

Vitrinite reflectance ( $R_o$ ) and ROCK-EVAL ( $T_{max}$ ) hydrocarbon (HC) maturity indices (MI), developed in petroleum geochemistry studies, can be used to estimate the maximum temperatures to which a rock has been buried, referred to as a hydrocarbon's "rank." Prior scientific study of the Williston Basin (Scattolini, 1977; Majorowicz et al., 1986, 1988; Price et al., 1984; Price 1996) all inferred or directly measured high paleogeothermal conditions. The Scattolini and Majorowicz work used thermal conductivity estimates of  $4 \text{ cal cm}^{-1} \text{ deg}^{-1} \text{ sec}^{-1}$ , or about  $2.4 \text{ W m}^{-1} \text{ K}^{-1}$ , for the Pierre Formation Shale (Combs and Simmons, 1973). However, the value that should have been used was closer to  $1.0$  to  $1.2 \text{ W m}^{-1} \text{ K}^{-1}$  (Gosnold, 1990). Price et al. (1984) produced  $R_o$  profiles versus depth and Total Organic Carbon (TOC) data suggesting high to extreme temperatures once existed in the Williston Basin. In addition to the argument that higher temperatures once existed in the basin, it has also been suggested by Price, based upon the same lines evidence, that the higher temperatures must have occurred in the Eocene or younger time frame. It is also acknowledged that the present-day burial temperatures are lower than those that are postulated to have once existed. As a result of these observations, some scientists have concluded that the previously existing conditions of the Williston Basin, i.e. the elevated temperature and heat flow conditions, are responsible for the volume of oil and gas resources existing, when compared to

reasonably similar basins with hydrocarbon source systems that have not experienced those same conditions. A full discussion of how higher temperatures in the Williston Basin would result in a higher volume of HC resources being generated when compared to that observed in other similar sedimentary basins goes beyond the scope of the present study; those interested can read more in the work of Price and others.

However, as evidenced by the work available to date by those attempting to computationally model the Williston Basin, assumptions have been made that are not in congruence with the findings of other researchers. Specifically, those modelers have assumed that heat flow in the Williston Basin was constant over geologic time (Gosnold and Huang, 1987; Gosnold, 1990; Burrus et al., 1995, 1996). The findings of Burrus et al. (1995; 1996), particularly, led to the development of two potential heat flow conditions experienced by the Williston Basin in the past, both of which were much lower than the expectations of other investigators. As such, objections have been raised about the work of the geophysicists attempting to create these previously simulated models. Concession was made for the fact that, to date, the computational processing capability could not match the needed complexity for a model of the system of interest.

In summary, the findings of Price et al. (1984; 1996) and Majorowicz et al. (1986; 1988) are in conflict with the findings of Burrus et al. (1995; 1996) and other previous works. The obvious question arises of what geologic event took place to cause such conditions to result. That particular question has been the source of as much speculation as the controversy concerning the resulting elevated heat flow conditions. While some of the speculation will be addressed in the discussion of this project, the ability to answer such a question also extends beyond the scope of so simple a study. More work will be

required to better address every parameter requiring study to the appropriate level of detail before any definitive statements can be made about such broad and encompassing topics.



## **CHAPTER II**

### **PROJECT INTRODUCTION**

#### **Overview**

The Williston Basin represents a unique opportunity for scientific investigation and economic development. A large sample base of rocks drilled from every well within the North Dakota boundaries is housed by the North Dakota Geological Survey (NDGS) due to laws passed during the 1950s. However, in spite of this enormous resource available for study and the impetus to understand the conditions present in a structurally simple sedimentary basin, science has still not yet developed a consensus message about the Basin's paleogeothermal conditions, their causes, and the implications thereof. Controversy remains in the scientific literature concerning the paleogeothermal and heat flow conditions of the Williston Basin. A full discussion of the implications of higher temperatures existing in the Williston Basin and how those conditions came about goes beyond the present study. The intention of this study is to address the previous work done by geologists and geophysicists to perform simulation models of the region. We intend to generate geophysical evidence that updates the work of previous researchers which addresses the specific grievances of other investigators concerning the assumption of constant heat flow through time.

## **Statement of Hypothesis**

It has been argued that previously attempted 1-D temperature models based on present day heat flow values do not explain the thermal maturity conditions experienced by the Williston Basin because those models have assumed constant heat flow through time. The argument made also contends that a thermal event must have taken place in the Eocene Epoch or younger time period. The present study will perform those suggested updates to computational models and combine those data with thermostratigraphy data. We hypothesize that our thermostratigraphy analysis and updated models and data will indicate that elevated heat flow could have existed in the Williston Basin at some time in the geologic past. However, we further hypothesize that the time frame suggested is incorrect and anticipate that our models will show the time frame necessary for a successful model could be much older than the Eocene. If the models are successful, they will indicate two things: 1) variable heat flow resulting from a thermal pulse event and allowed to equilibrate over time could have resulted in present day heat flow, and 2) the variable heat flow could be modeled to begin before the Eocene Epoch, such as the Cretaceous, and still result in present day heat flow.

## **Study Setting**

The Williston Basin (WB), centered in the western half of North Dakota (ND) near the border with Montana, is an intracratonic basin that extends into parts of southwestern Saskatchewan, southeastern Manitoba, eastern Montana, and western North Dakota (Ricker, 2015). Figure 1 (Ricker, 2017; modified from Gerhard et al., 1982) demonstrates the extent of the Basin as well as some of the major structural features in the region as well. Beyond the extent of the Basin lie the Sioux Uplift, the Punnichy

Arch, and the Sweetgrass Arch. Structurally, the Williston Basin is considered the simplest sedimentary basin the world, with little to no major and only minor faulting and mostly flat-lying sediments (Price, 1996). Such conditions are, in fact, one of the major reasons why a deep understanding of the temperature and heat flow conditions in the Basin and the history thereof are of profound significance. Within North Dakota are found the deepest and most economic elements of the Basin.

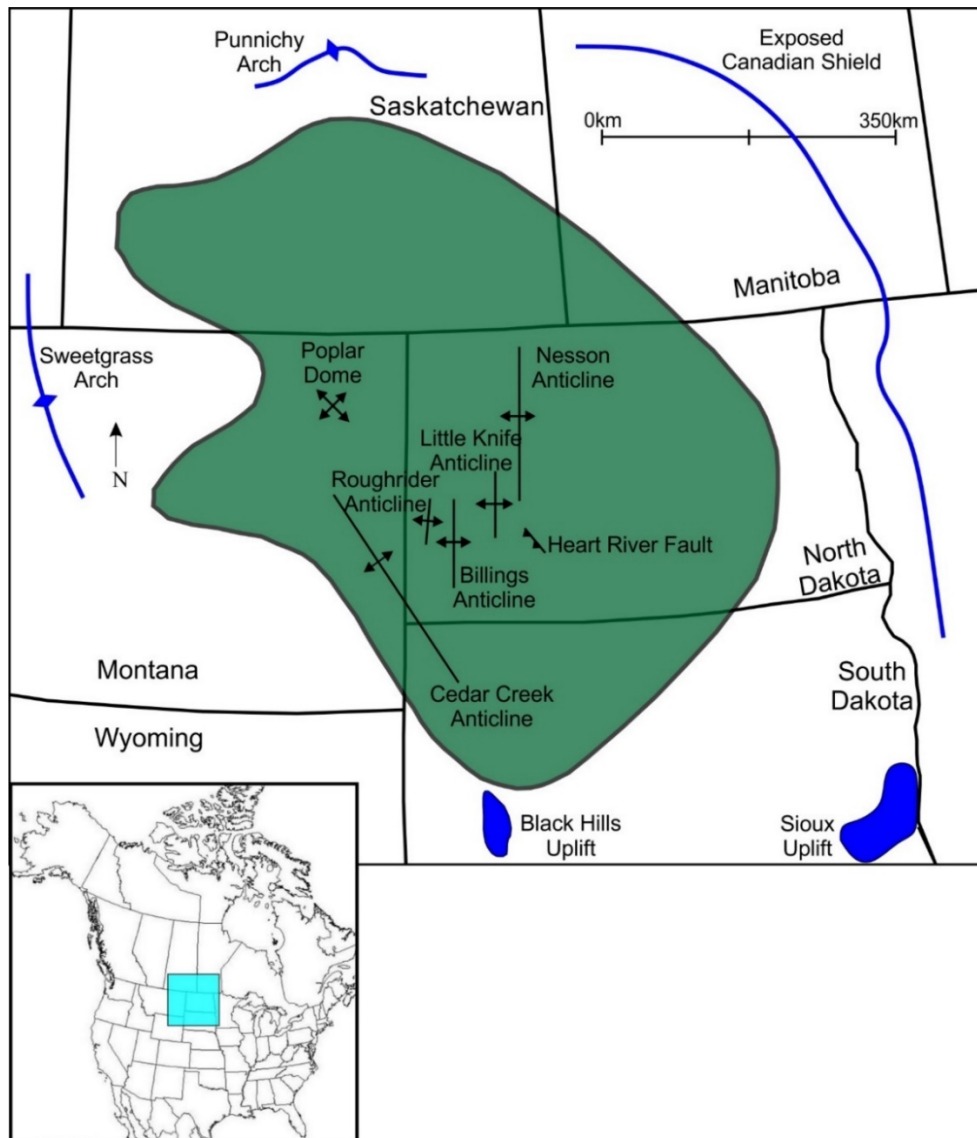


Figure 1. Location and outline of the Williston Basin showing major basement structures. (used with permission of Faye Ricker, 2017; modified from Gerhard et al., 1982).

Table 1 (modified from Murphy et al., 2009) shows the chronological order of the Basin's sequence stratigraphic column with accompanying ages and approximate timespans. Present day conditions show evidence for sedimentation occurring in the region from Cambrian to the Early Tertiary with the Fort Union Group (Price, 1996). Further, evidence also shows, in the form of unconformities, the occurrence of nondeposition and/or basin uplift and erosion (Price, 1996). As such, it can be problematic to determine exactly what extent of sedimentation took place above the Cretaceous Pierre Formation Shale. Heck et al. (2002) determined that the structure shows evidence of initial subsidence during the Ordovician. A suite of transgressive and regressive sequences indicates shallow marine environment occurrence (Poter, Price, and McCrossan, 1982). Generally, the Williston Basin contains 1 to 2 km of clastic rocks Cenezoic to Mesozoic in age overlying approximately 2 to 3 km of carbonates Paleozoic in age. Sloss (1963) developed a set of sequence subdivisions that are still mostly used to this day when describing the sequence stratigraphy of the area. Six major unconformities occur within the Basin, which would suggest times of regression maxima (Sloss, 1963). The six subdivisions are described by Sloss (1963) in the following manner: the late Precambrian Sauk Sequence, the early the early Middle Ordovician Tippecanoe sequence, the early Middle Devonian Kaskasia sequence, the "Post Elvira" Mississippian Absaroka sequence, the early Middle Jurassic Zuni Sequence, and the Late Paleocene Tejas sequence. The Paleocene to Upper Cretaceous rocks are a series of lignites, siltstones, shales, and sandstones. The Lower Cretaceous rocks are primarily shales with sandstones found in the Newcastle and Inyan Kara Formations. Jurassic to Upper Mississippian rocks are comprised of marine-derived shales, siltstones, sandstones,

limestones, dolomites, and evaporites. Dense, thick limestones make up the Middle to Lower Mississippian rocks. Lower Mississippian to Middle-Upper Devonian rocks, comprised of shales, sandstones, siltstones, limestones, dolomites, and evaporates. The strata at those particular depths have long been the subject of intense scientific investigation and economic development. Middle-Upper Devonian to Cambrian rocks are composed primarily of dolomites and limestones, with lesser amounts of shales, sandstones, and evaporites. Interestingly, the oils from these Lower Paleozoic rocks are compositionally different from Bakken shale oils, but such is not considered further in the current study (Price, 1996).

Table 1. Formations of the North Dakota stratigraphic column with average thermal conductivity measurements (modified from Murphy, 2009; Gosnold, et al., 2010).

Age	Years (mya)	Formation	Thermal Conductivities
Quaternary	2.6	Surface	N/A
Tertiary		Brule Fm	1.2
Tertiary		Chadron Fm	1
Tertiary		Golden Valley Fm	1.1
Tertiary		Tongue R. Fm	1.1
Tertiary		Slope Fm.	1.1
Tertiary		Cannonball Fm.	1.1
Tertiary	65	Ludlow Fm	1.1
Cretaceous		Hell Creek Fm	1.1
Cretaceous		Fox hills Fm	1.2
Cretaceous		Pierre Fm	1.1
Cretaceous		Niobrara Fm	1.3
Cretaceous		Carlille Fm	1.2
Cretaceous		Greenhorn Fm	1.2
Cretaceous		Belle fourche Fm	1.2
Cretaceous		Mowry Fm	1.2
Cretaceous		Newcastle Fm	1.3
Cretaceous		Skull Creek Fm	1.2
Cretaceous	145	Inyan Kara Fm	1.6
Jurassic		Swift Fm	1.2
Jurassic		Rierdon Fm	1.6
Jurassic	201.6	Piper Fm	1.6
Triassic/Permian	251	Spearfish Fm	1.6
Permian		Minnekahta Fm	2.5
Permian		Opeche Fm	1.2
Permian	299	Broom Creek Fm	2.2
Pennsylvanian		Amsden Fm	4
Pennsylvanian	318	Tyler Fm	2.7
Mississippian		Otter Fm	2.7
Mississippian		Kibbey Fm	2.7
Mississippian		Charles Fm	2.49
Mississippian		Mission Canyon Fm	2.49
Mississippian		Lodgepole Fm	2.49
Mississippian/Devonian	359	Bakken Fm	1.1
Devonian		Three Forks Fm	1.3
Devonian		Bird Bear Fm	3.13
Devonian		Duperow Fm	3.19
Devonian		Souris R. Fm	2.92
Devonian		Dawson Bay Fm	2.75
Devonian		Prairie Fm	4
Devonian	416	Winnepegosis Fm	2.99
Silurian		Interlake Fm	3.77
Silurian/Ordovician	444	Stonewall Fm	3.89
Ordovician		Stony Mountain Fm	3.79
Ordovician		Red River Fm	3.28
Ordovician		Winnipeg Fm	4.07
Ordovician		Erosion	3.5
Ordovician/Cambrian	488; 542	Deadwood Fm	3.46
Precambrian	4600	N/A	N/A

## **Thermal Energy Generation and Flow in the Earth's Crust**

Heat transfer is a branch of science and engineering concerned with the study and use of the generation and exchange of thermal energy, or heat, within and between physical systems. One example of these principles commonly discussed is pictured as a person holding a pot of water, via a handle, over a fire. The fire produces thermal radiation energy, which is transferred to the pot. The water contained within the pot experiences convection as boiling occurs; thus, heat is transferred. Finally, conduction takes place through the pot itself, as some of the radiated heat is transferred through the solid material of the pot, eventually reaching the handle that the person is holding. The major mechanisms of heat transfer within the Earth are thermal conduction, thermal convection/advection, and thermal radiation. These mechanisms often occur simultaneously throughout any physical system in question.

Heat contained in the Earth develops from both internal and external sources. While some internal heat is the result of "original heat," or heat trapped during Earth's early formation stages, heat is derived primarily via convection and conduction of the mantle (approximately 60% contribution) and decay of unstable radiogenic isotopes  $^{232}\text{Th}$ ,  $^{235}\text{U}$  and  $^{238}\text{U}$ , and  $^{40}\text{K}$  (approximately 40% contribution) (Pollack, 1982; Beardsmore and Cull, 2001). Early studies in radiogenic heat generation involved an attempt to determine a means of calculating its contribution to heat flow, which led scientists to develop the concept of "heat flow provinces" (Roy, Decker, Blackwell, and Birch, 1968). Heat flow provinces are delineated areas that contain relatively uniform lower crust and upper mantle heat flow and consistent thickness of the radiogenic heat generation layer. These areas are the result of a common tectonothermal geologic

history. For instance, the Northern Great Plains, where the Williston Basin is located, is an area that is assigned to the “Eastern US” heat flow province (Roy, Blackwell, and Birch, 1968). The work of both of these studies led to the understanding of a linear relationship between heat generation and heat flow (Lachenbruch, 1968; Roy, Blackwell, and Birch, 1968):

$$Q = q + A_0D \quad \text{Equation 1.}$$

where:

$Q$  is surface heat flow ( $\text{W} \cdot \text{m}^{-2}$ )

$q$  is a constant component of heat flow from the mantle ( $\text{W} \cdot \text{m}^{-2}$ )

$A_0$  is radioactive heat generation or production ( $\mu\text{W} \text{m}^{-3}$ )

$D$  is thickness of the radiogenic heat producing layer (m)

Any further discussion of the Earth’s heat generation mechanisms is beyond the scope of the present work and better left to other such studies (see Ricker, 2015).

The Earth’s internal surface (crustal) temperature increases with depth at a rate of approximately  $30^\circ\text{C}$  per kilometer (Lund et al., 2008). "Terrestrial heat flow is defined as the quantity of heat escaping per unit time from the Earth's interior across each unit area of the Earth's solid surface (Pollack, 1982)." Heat advection usually occurs in localized areas of the crust where significant fluid flow allows for such a transport process, either through porous and permeable lithologies or via secondary structural deformation processes such as faults. While heat is moved through much of the earth by convection (i.e. in the mantle) (Beardsmore and Cull, 2001), heat conduction is the primary heat transport process at work in the Earth’s crust (Clauser, 2009).

### **Thermal Conduction**

Heat conduction is the transfer of internal energy by progressive microscopic vibration and collision of particles within a body or through a boundary between two



bodies (Cengel and Ghajar, 2015). The rate of heat transfer via conduction is a function of the temperature difference, or gradient, between the two bodies and the properties of the conductive medium through which the heat is transferred. This principle is summarized by Fourier's Law of Heat Conduction:

$$q = \frac{dT}{dz} \lambda \quad \text{Equation 2.}$$

where:

$q$  is the local heat flux density ( $\text{W}\cdot\text{m}^{-2}$ )

$\frac{dT}{dz}$  is the temperature gradient ( $\text{K}\cdot\text{m}^{-1}$ )

$k$  or  $\lambda$  is the material's conductivity ( $\text{W}\cdot\text{m}^{-1}\cdot\text{K}^{-1}$ )

The present study makes use of the  $\lambda$  convention. Thermal conduction is, thus, a form of diffusion, where heat spontaneously flows from hotter to colder regions, as described by the Second Law of Thermodynamics (Cengel and Ghajar, 2015).

### **Steady State Thermal Conduction**

Steady state conduction is achieved when the temperature differences driving conduction are constant. As the system is allowed proceed with the thermal equilibration, the spatial distribution of temperatures achieved, or temperature field, does not change. The amount of heat entering any defined space of the system equals to amount of heat exiting the same space. Mathematically, we say all partial derivatives of temperature at any point with respect to time must be zero, irrespective of partial derivatives with respect to space (Cengel and Ghajar, 2015).

With respect to Fourier's Law, steady state conduction can be thought of in two equivalent forms: the integral form, in which the system is considered as a whole, and the differential form, in which heat flow of the system can be considered locally (Cengel and Ghajar, 2015). In the differential form, steady state heat conduction is described as in the

above equation and heat flow is occasionally referred to as local heat flux density, or  $\rightarrow q$  in other disciplines of science and engineering. Thermal conductivity is typically treated as a constant, although this is not always true in natural conditions. For instance, the assigned thermal conductivity values typically vary with orientation in anisotropic materials (Dr. I-Hsuan Ho, personal communications) and spatially in non-uniform materials (Crowell, J, 2015).

### **Factors of Elevated Geothermal Gradients and Heat Flow**

Various phenomena, such as crustal thickness, water advection, and localized radioactivity can affect regional heat flow values (Lachenbruch, 1970). Heat production of plutonic rocks has been demonstrated to exponentially decrease with crustal depth (Lachenbruch, 1970). Blackwell (1971) also argues "local variability of heat flow in crystalline terrain is due primarily to lateral variations in upper crustal heat production," causing a linear relationship between heat flow and heat production to exist in plutonic rocks. This relationship is demonstrated in Equation 1. Thinner crusts tend to yield a higher heat flow, and a thermal boundary layer develops as crust ages and thickens (Crough, 1976). Sclater et al. (1980) also detail how geologic history affects regional heat flow by arguing that surface heat flow is influenced by distribution of heat-producing elements, as well as the last orogenic event in the area and possible erosion that occurred. According to Morgan (1984), quantity and distribution of heat producing elements in the lithosphere are the main factor controlling temperature distribution and surface heat flow. Furthermore, variations in lithospheric thickness also directly impact thermal regime (Morgan and Gosnold, 1989).

## **CHAPTER III**

### **METHODS**

#### **Overview**

In this chapter, an explanation for measuring temperature at depth is presented first. Following an explanation of thermostratigraphy data generation, a brief explanation is provided for the use of the T-z projection plots for determination of geothermal gradient. This chapter then concludes with the methods used to create the heat flow simulation models under steady-state conditions necessary for the present study.

#### **Thermostratigraphy**

A number of scientists have previously used thermostratigraphy in order to model geothermal conditions present in sedimentary basins (Lachenbruch; 1970; Gosnold, 1984, 1991, 1999; Gosnold et al., 2010; Crowell and Gosnold, 2011; Crowell et al., 2011; Gosnold et al., 2012). The studies conducted using thermostratigraphy demonstrate the constraining power of this methodology. Initially, Lachenbruch (1970) was concerned with the linear heat flow relationship, where crustal temperature and heat production are concerned. In 2011, Gosnold et al. used this methodology to argue that present day heat flow is underestimated in regions near the Pleistocene ice margin, due to a transient climate signal that disturbs the geothermal gradient. Most importantly, the correlation of calculated projections to the correctly measured data of the same area shows that

thermostratigraphy is a methodology for determining the thermal structure of a region when certain types of data are available.

Previously, Fourier's Law of Heat Conduction has been discussed (Equation 2) which makes it possible to determine a value of heat flow, given the geothermal gradient and thermal conductivity are known. If the expression is rewritten as  $\frac{dT}{dz} = \frac{q}{\lambda}$  and solved for temperature, T, this simple rearrangement leads to the basic expression of thermostratigraphy. The temperature at any depth, T(z), can be calculated (Gosnold, 1984, 1991, 1999, 2012) by:

$$T_z = T_0 + \frac{qz_i}{\lambda_i} \quad \text{Equation 3.}$$

where:

$T_0$  is surface temperature (K)

$q$  is surface heat flow ( $W \cdot m^{-2}$ )

$z_i$  and  $\lambda_i$  are the thicknesses and thermal conductivities, respectively, of the *ith* Stratum (m;  $W \cdot m^{-1} \cdot K^{-1}$ )

However, in order to create a meaningful thermal profile that accounts for all depths and/or strata, it is important that the equation contain another term. Thus, the equation can be slightly modified with a Sigma notation in order to indicate that the calculation must be iterated across all n preceding depth intervals:

$$T_z = T_0 + \sum_{i=1}^n \frac{qz_i}{\lambda_i} \quad \text{Equation 4.}$$

The resulting dataset is plotted as a temperature versus depth curve, or T-z plot, thus creating the desired thermal profile. The equation has been referred to as TSTRAT by Gosnold (2012).

It is possible to then use the resulting T-z plot profile in order to determine geothermal gradient at depth. The geothermal gradient is simply the change in temperature,  $dT$ , divided by the change in depth,  $dz$ . Applying the equation of a line to the profile will provide this information, and a simple hand calculation for any temperature-depth interval can do the same.

Well data gathered from the NDIC database of oil & gas industry drilling operations in North Dakota (Figures 2 and 3), data used in previous work, can be used to perform the TSTRAT analysis needed for this study. NDGS wells #25, #527, #607, #2010, #2615, #6464, #6616, #7020, and #7783 were chosen for the present study, as these are the same wells used in previous study of the topics central to this issue (Price, 1996).

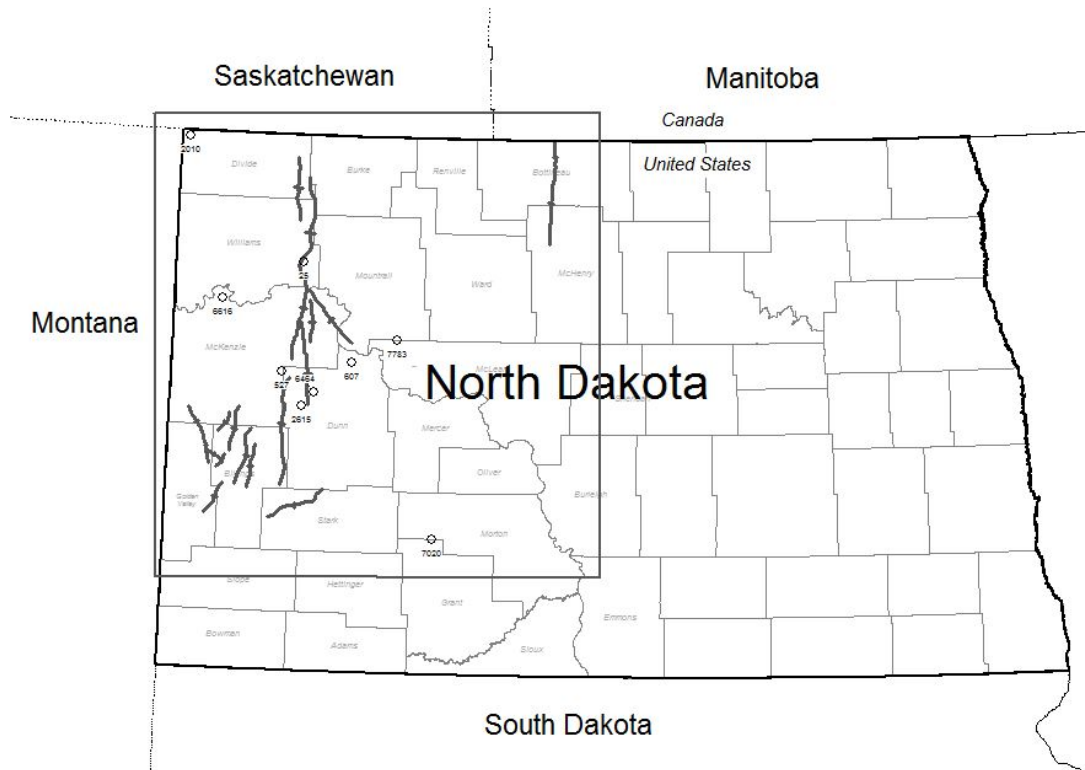


Figure 2. Location and outline of the study area within western North Dakota. Map created using PETRA software.

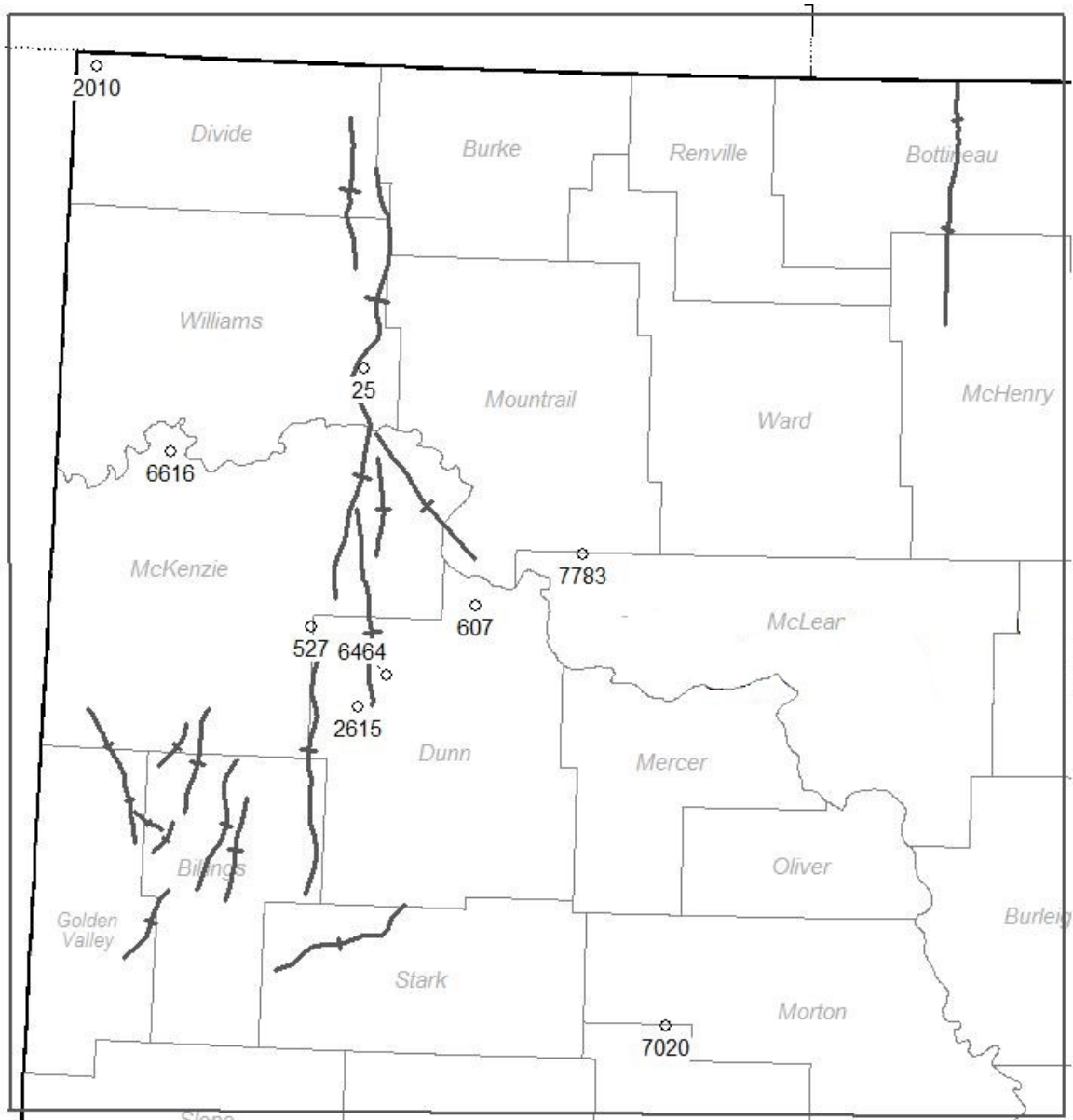


Figure 3. Locations of wells used in the present study. Map created using PETRA software.

To begin, the process involves the simple input of formation top data into Microsoft Excel. The depth information is then used to compute the remaining formation tops, employing a technique that involves extrapolation and any necessary depth adjustment. Once all formation tops, known and computed, are gathered, the thicknesses of each formation are known through a simple subtraction calculation. After the complete

formation thickness dataset is determined, the TSTRAT equation is applied using previously determined thermal conductivity values for each formation, regional heat flow values obtained from previously published scientific literature, and surface temperatures in order to generate the desired T-z profiles. For this study, the heat flow values were obtained from the recent results of Mark McDonald (2015), seen in Figure 4.

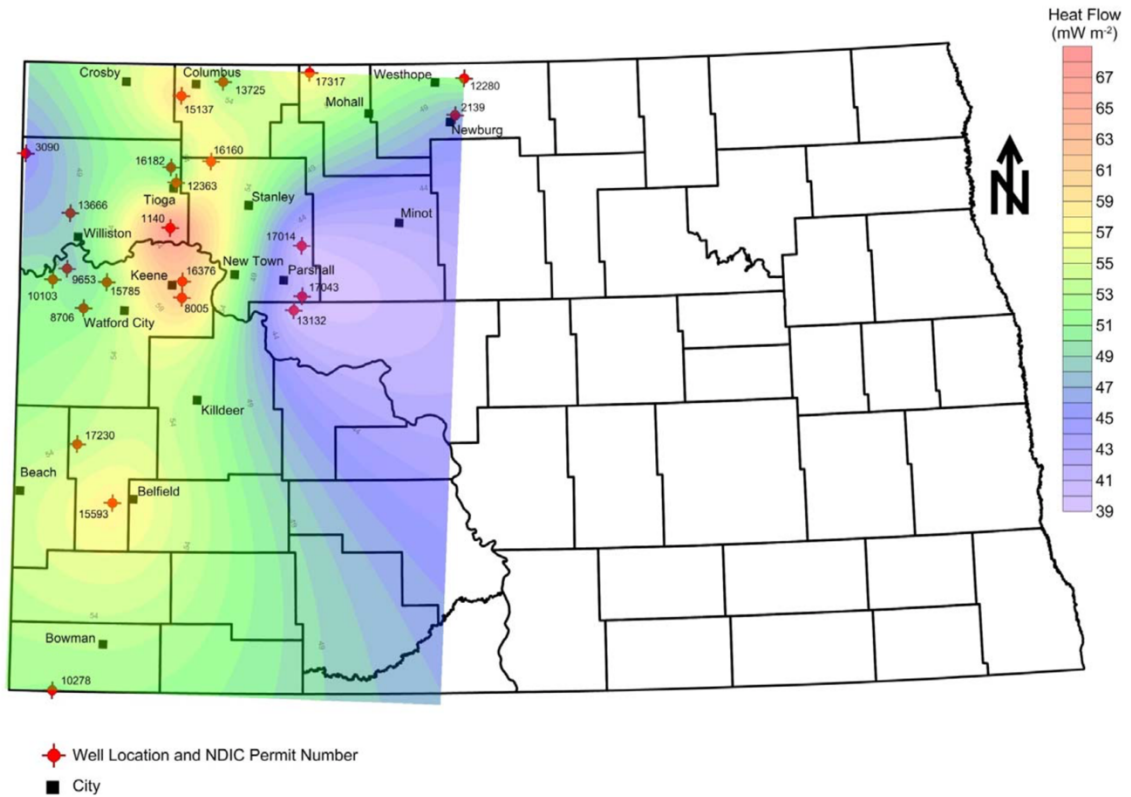


Figure 4. Mean heat flow values occurring within the area of study (used with permission of the NDGS; McDonald, 2015).

### Steady State Conductive Heat Flow Modeling

In any heat flow modeling software solution, a high degree of control is administered by the user because individual values can be altered as needed. Cengel and Ghajar (2015) argue that people are unlikely to write their own programs to solve such problems and should, instead, rely on more professional software packages that are “well-

established,” meaning tested by many users. They further argue that others are less likely to be skeptical of results obtained from such commercial software. Despite the fact that a number of other software solutions exist to accomplish steady-state heat flow modeling, Dr. William Gosnold’s Finite Difference Heat Flow Simulation (v. 2.5.4), or “ARC,” software offers the advantages of being developed by the researchers performing the present study and is, thus, highly modifiable for the user’s needs. The software was written in originally Fortran and converted to C++ programming language by David Apostol of the Department of Computer Science at the University of North Dakota. Based on another software solution developed by Charles Brott (1978), ARC was developed in order to perform finite difference determination of steady-state heat flow by calculating temperature and heat generation for a given system subdivided into cells and heat transfer to and from surrounding cells (Crowell, J, 2015). The ARC modeling solution helps address questions relating to geothermal conditions of crustal evolution over some duration of geologic time, but others have demonstrated its usefulness for other systems requiring a modeling scheme as well, such as Crowell 2015. Indeed, ARC allows for ease in modeling numerous heat transfer processes.

In order to perform the analysis, a system is modeled using ASCII format input codes and desired values of system parameters in a Microsoft Excel file. Thermal conductivity, radiogenic heat production, basal heat flow, heat capacity of rock and fluid, density, advection constraints, starting temperatures, velocity, direction and cell size and model dimensions can each be specified in the desired system model. The model file is read, interpreted, and executed by the ARC software, demonstrated in Figure 5. The software uses the mathematic principles it is written to perform to carry out a step-wise



determination of heat flow throughout the system, approximately once every two simulated minutes, over a specified period of model duration. Post-simulation results are saved into a data file that can be visualized and reported using Golden Software's Surfer and Voxler software application packages.

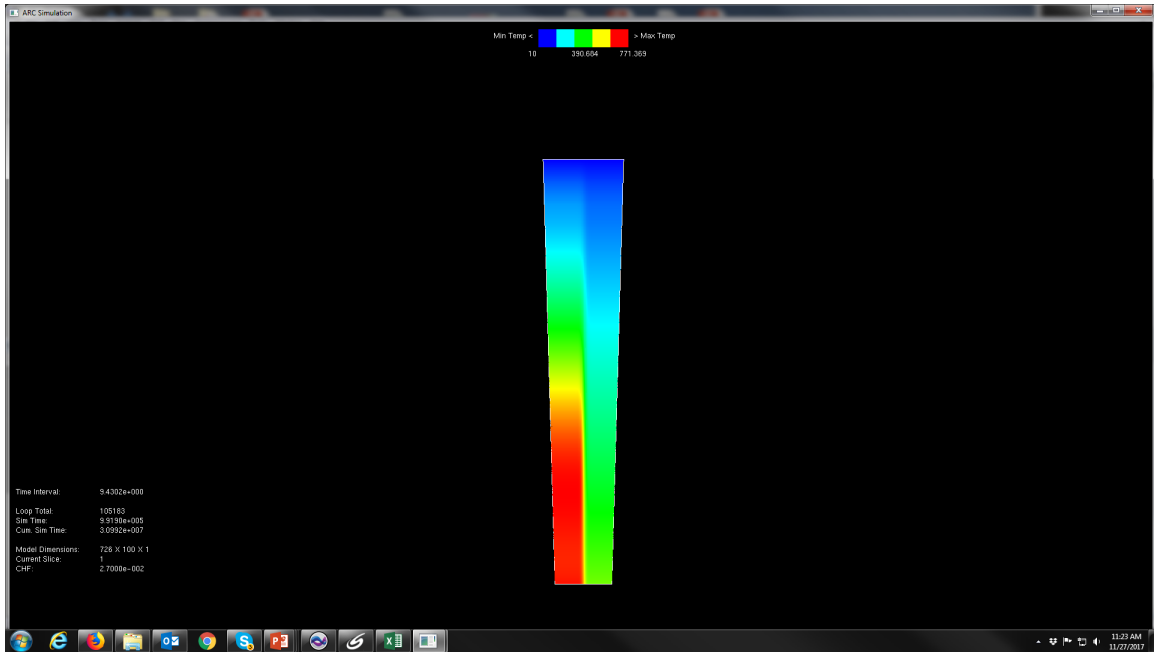


Figure 5. Computer screen capture of an ARC model simulation in progress.

A model of a transect of the Williston Basin was developed for this study. We developed a model that shows a 3650 km thick x 400 km wide section of the Earth, which accounts for the uppermost crust to a portion of the outer core. The Earth's uppermost 6 km of crust was modeled using 8 harmonic mean thermal conductivity values calculated using data previously developed for NDGS well #2894. Harmonic mean thermal conductivity values were used in order to simplify the model creation process. The system was designed to use a base heat flow value of  $27 \text{ mW m}^{-2}$  entering the crust from the mantle, in congruence with previous study determinations of basement heat flow contribution values. One variable heat flow zone, a 20 km thick x 200 km wide block

located 20 km below the surface, was established to simulate a magma lens intrusion resulting from a rifting event, such as that observed in the Rio Grande Rift event. The simulation was designed to begin with present day heat flow conditions, as though the same conditions existing today also existed at the time period beginning each model. The model developed was set to run for 35 my and 65 my, roughly correlating the beginning of the Eocene Epoch and the end of the Cretaceous Period, respectively.

Once the model is generated in Excel, the ARC software is initiated and the prompts followed. The software prompts for the user to input choice of whether or not to visualize the simulation, model file name, a file name(s) to use for results reporting, desired iteration time-steps, simulation duration, and screen update frequency.

Any model of steady state heat conduction that results in a discrete, numerical formulation can be performed by multiple methods, such as finite difference, finite element, boundary element, and energy balance (Cengel and Ghajar, 2015). The energy balance method and the finite difference method both result in the same set of algebraic equations being used. In the finite difference method, differential equations are replaced with algebraic equations, thus replacing derivatives with differences (Cengel and Ghajar, 2015). The ability to establish and maintain boundary conditions before and during model simulation and resulting temperature values being established for discrete points for all selected points in the system ensures the veracity of the model.

## **CHAPTER IV**

### **RESULTS**

#### **Overview**

The result of developing T-z plots using the principles of thermostratigraphy is that a demonstration of geothermal gradients and paleogeothermal conditions in Williston Basin can be achieved. The results also show the differences in the modeled basin when run for varying time durations.

#### **Thermostratigraphy**

The results generated from applying thermostratigraphy to formation top data of NDGS wells #25, #527, #607, #2010, #2615, #6464, #6616, #7020, and #7783 are shown in the following figures. The dots observed in each plot represent the temperature data calculated at each formation top. After the temperature data was generated, it was plotted using depth data. A simple fitting line was then applied, in order to more easily visualize the overall trend of the temperature profile.

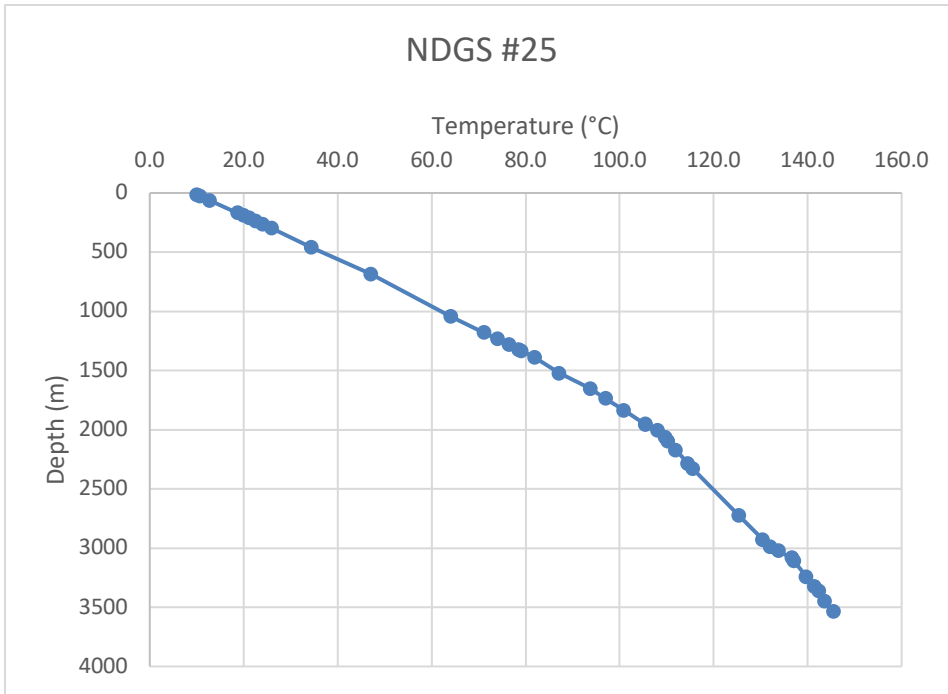


Figure 6. Plot of computed temperatures of NDGS #25. Computed temperatures are from Eq. 4 and are shown with depth information in Table 2 of Appendix A.

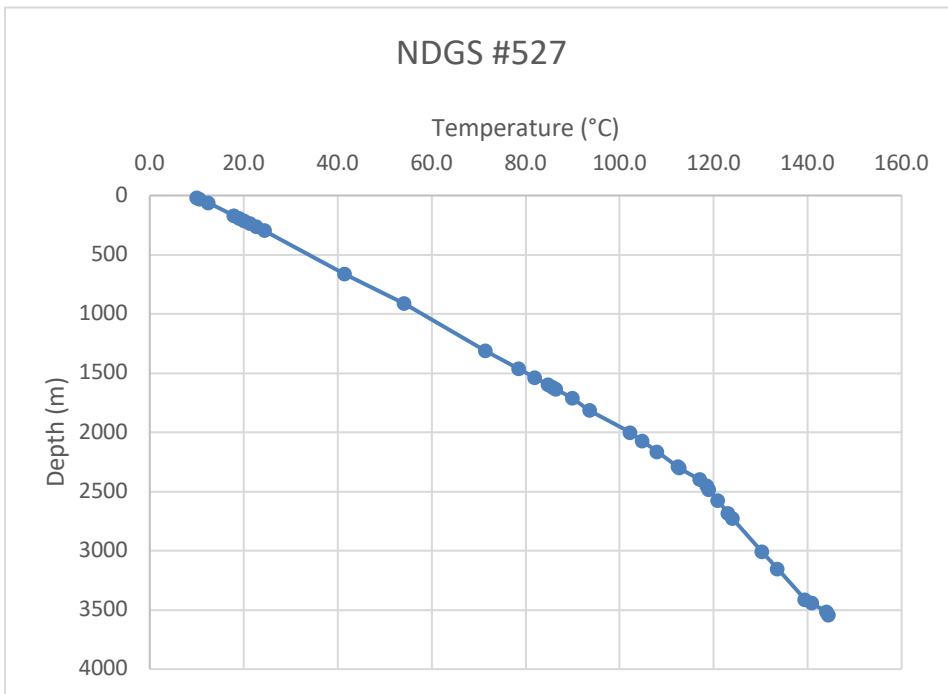


Figure 7. Plot of computed temperatures of NDGS #527. Computed temperatures are from Eq. 4 and are shown with depth information in Table 3 of Appendix A.

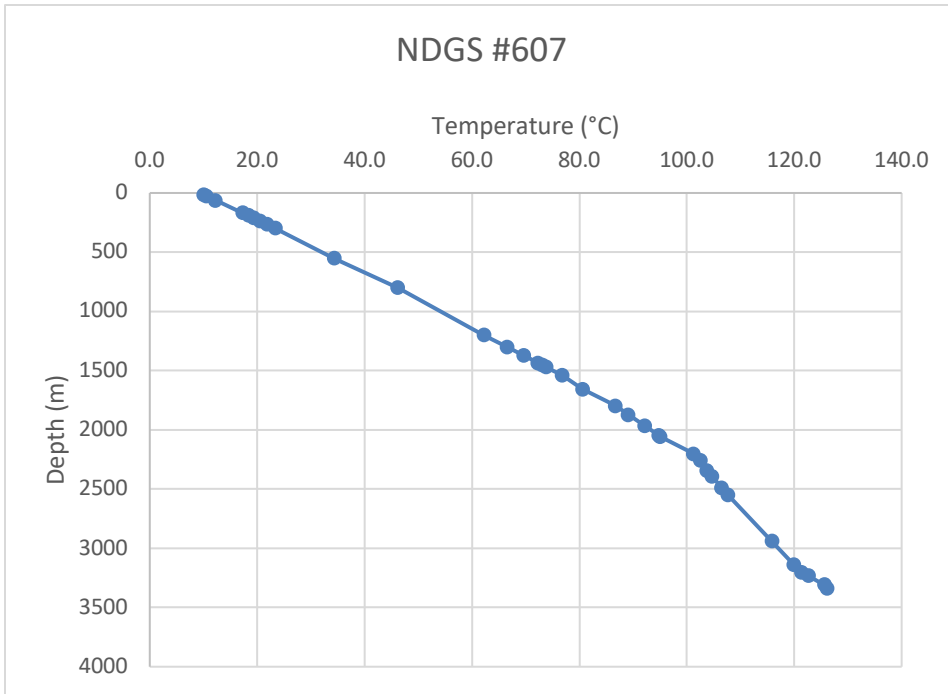


Figure 8. Plot of computed temperatures of NDGS #607. Computed temperatures are from Eq. 4 and are shown with depth information in Table 4 of Appendix A.

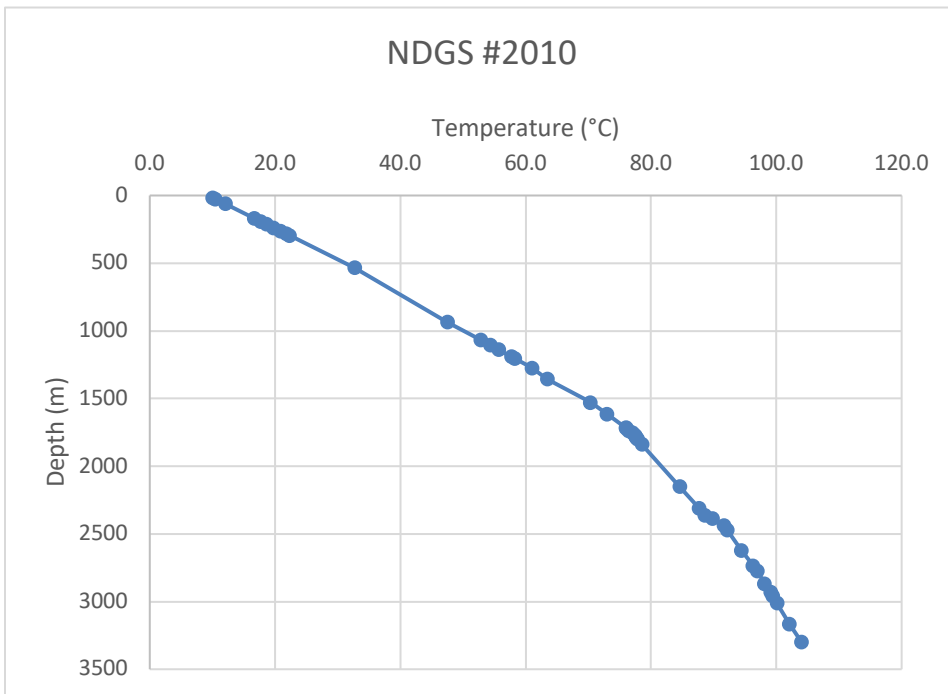


Figure 9. Plot of computed temperatures of NDGS #2010. Computed temperatures are from Eq. 4 and are shown with depth information in Table 5 of Appendix A.

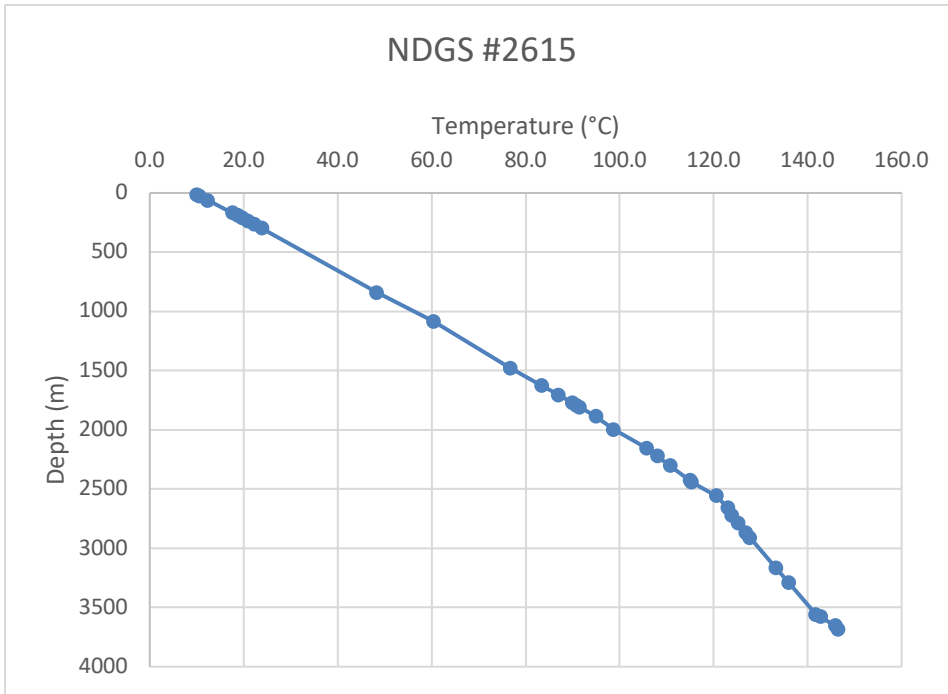


Figure 10. Plot of computed temperatures of NDGS #2615. Computed temperatures are from Eq. 4 and are shown with depth information in Table 6 of Appendix A.

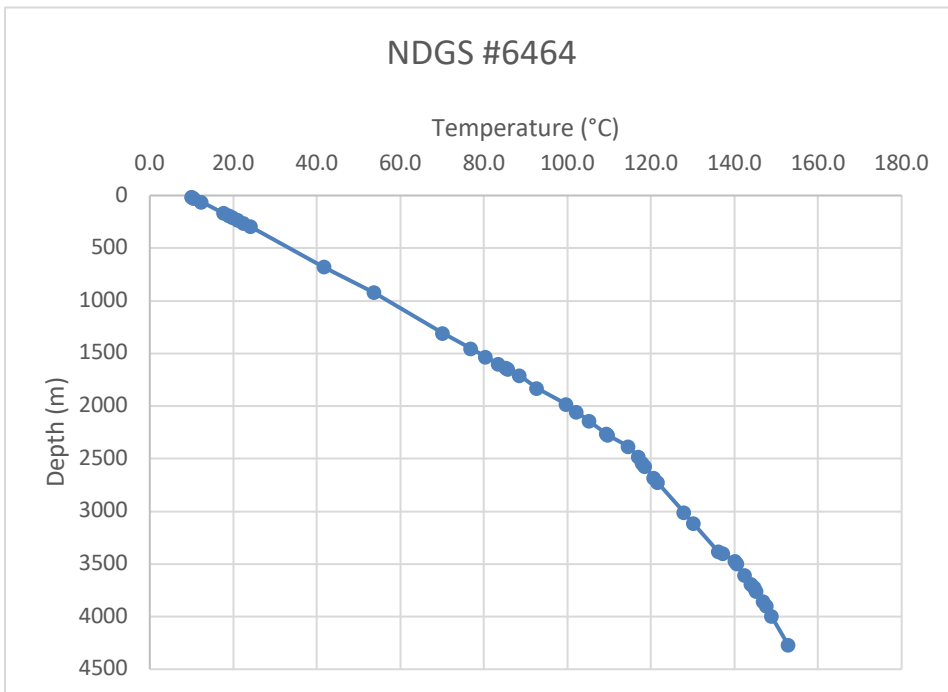


Figure 11. Plot of computed temperatures of NDGS #6464. Computed temperatures are from Eq. 4 and are shown with depth information in Table 7 of Appendix A.

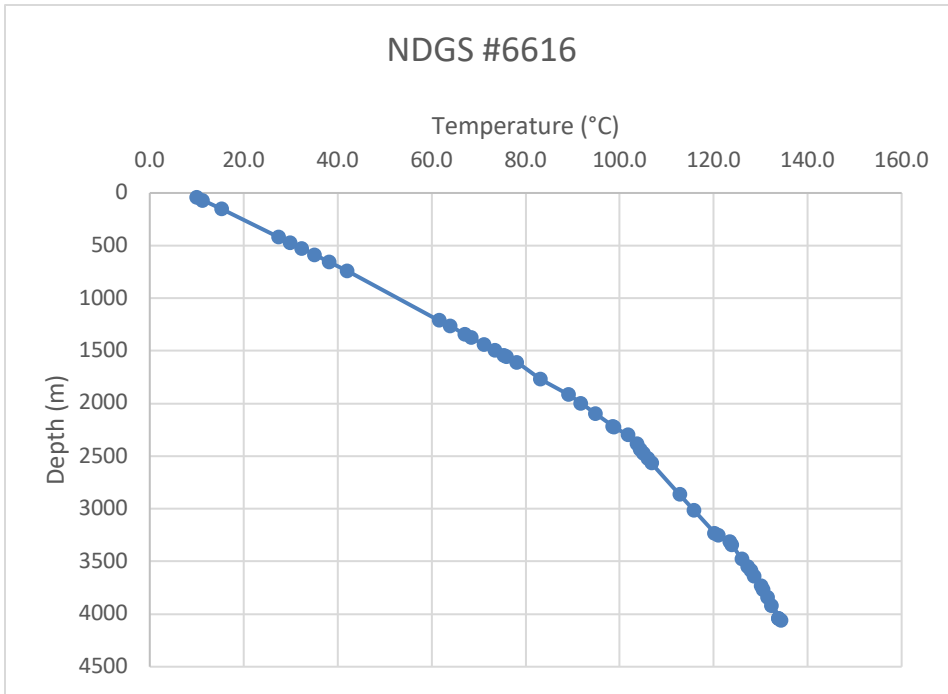


Figure 12. Plot of computed temperatures of NDGS #6616. Computed temperatures are from Eq. 4 and are shown with depth information in Table 8 of Appendix A.

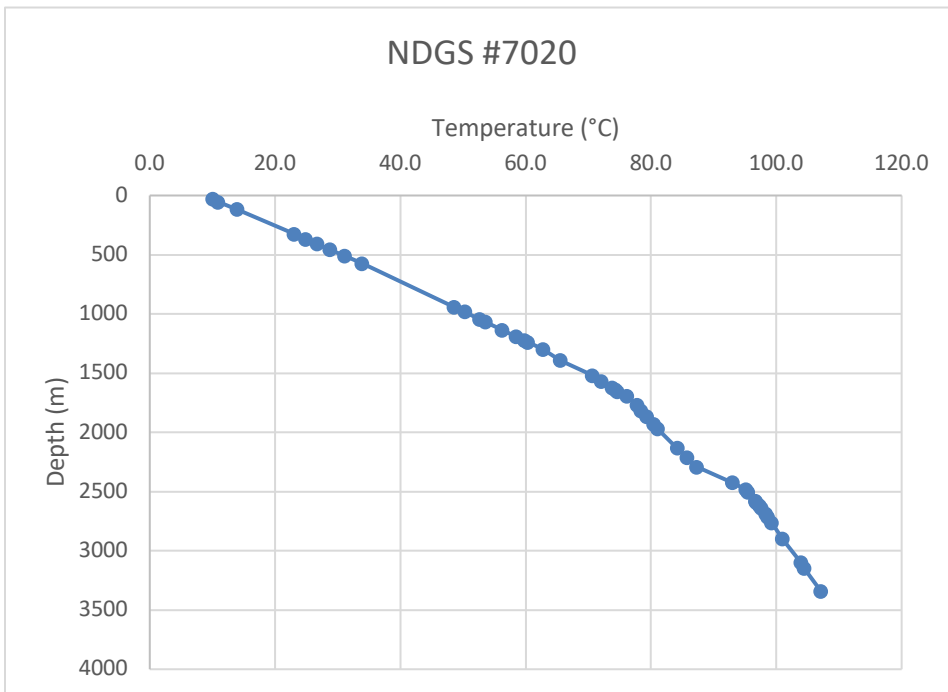


Figure 13. Plot of computed temperatures of NDGS #7020. Computed temperatures are from Eq. 4 and are shown with depth information in Table 9 of Appendix A.

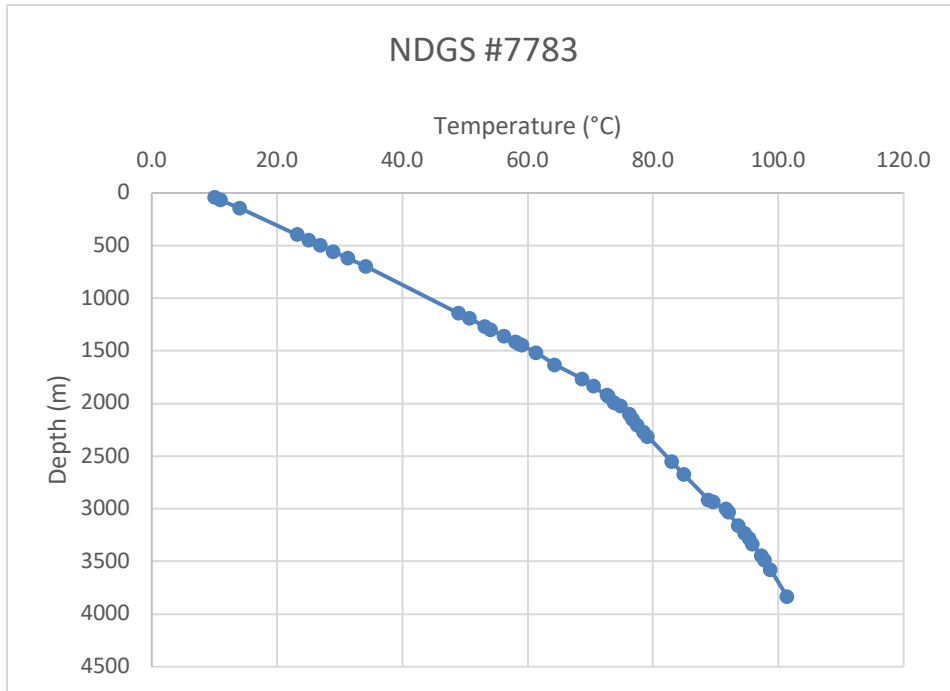


Figure 14. Plot of computed temperatures of NDGS #7783. Computed temperatures are from Eq. 4 and are shown with depth information in Table 10 of Appendix A.

Additionally, we chose to combine the TSTRAT datasets for all wells calculated in the present study into one chart, in order to more easily demonstrate the differences in temperature and geothermal gradient data from well to well. The same method used to generate the individual well plots was again used to generate the combined data plot.



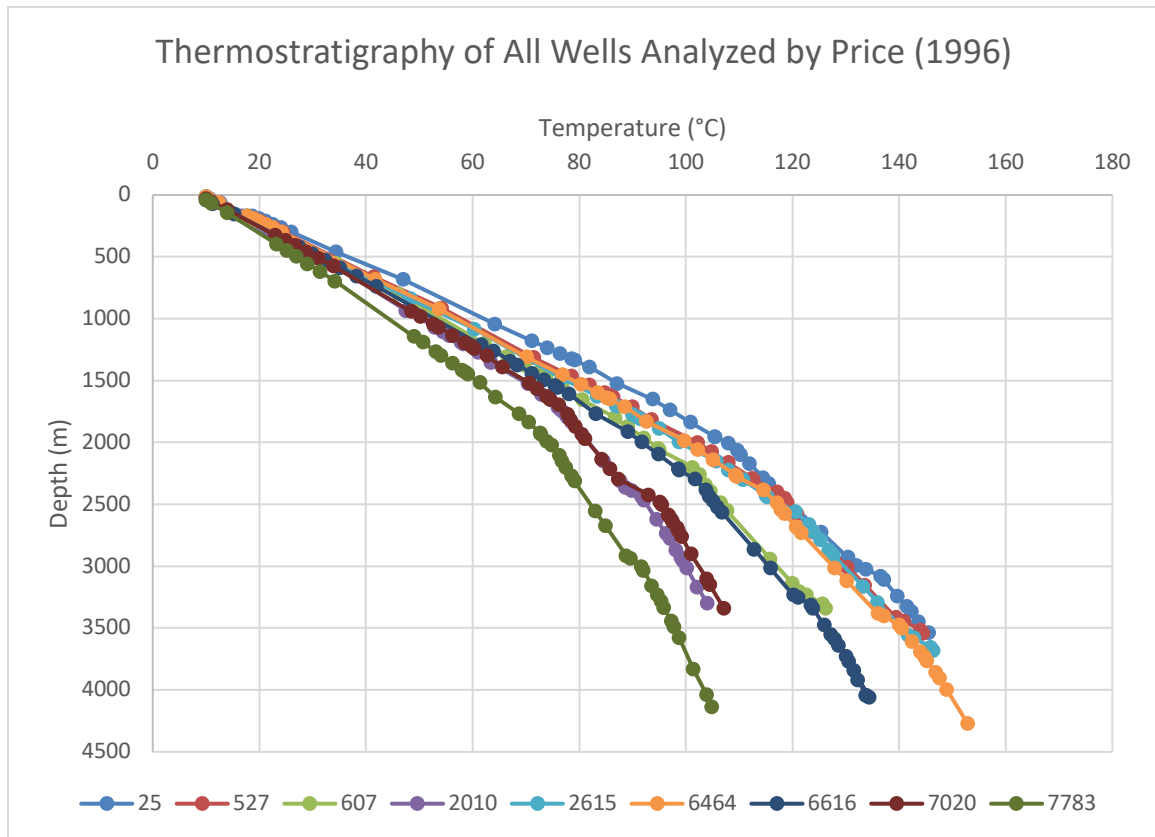


Figure 15. Plot of computed temperatures of all well used in this study. Computed temperatures are from Eq. 4 and are shown with depth information in Tables 2 - 10 of Appendix A.

The data generated in the present study highlight the same interesting geothermal feature that has been seen in TSTRAT and equilibrium well log profiles of numerous previous studies. The Williston Basin, generally, has a bimodal composition, with a 1 to 2 km thick layer of clastic rocks Cenezoic and Mesozoic in age overlying 2 to 3 km of carbonates Paleozoic in age (Gosnold, 2012). That feature is observable in the present datasets when, in each dataset at approximately 2km in depth, the gradient shown changes from a steep gradient to a shallow gradient. This marked change makes clear the importance of thermal conductivity values in the calculation of TSTRAT data.

If heat flow in the past were constant, all curves generated by the thermostratigraphy technique would overly one another. Clearly, these temperature

profiles do not do so. This would potentially indicate that heat flow input into the crust from the basement rocks must be variable across the basin or that the heat flow within the basin itself must be variable. While this dataset does not conclusively indicate that the heat flow throughout the basin has been variable in the past, the data indeed mirrors the findings of other researchers, such as Scattolini (1977), Majorowicz (1986, 1988), and Price (1984).

### **Steady State Conductive Heat Flow Modeling**

Finite difference heat flow simulation results of steady state conductive heat flow modeling are shown in the following figures. The first figure shows the results of a simulation designed to run for a duration of 35 my is displayed first, followed by a figure showing the results of the same simulation run for a duration of 65 my. Thermal conductivity, based on harmonic mean values calculated from NDGS well #2894 and others, is the vertical change parameter, and aerial distance in km is the horizontal change parameter.

A few simple verification calculations were done in order to briefly verify that the results obtained made logical sense in comparison to what is known about sedimentary basin geothermal conditions. For instance, the models run gave an output of values for basement heat flow that are consistent with those values demonstrated in previous scientific investigation.

The results from both simulations were contoured in order to highlight the equilibration of temperature and dissipation of the thermal event throughout the system modeled. Those results are shown in the following figure.

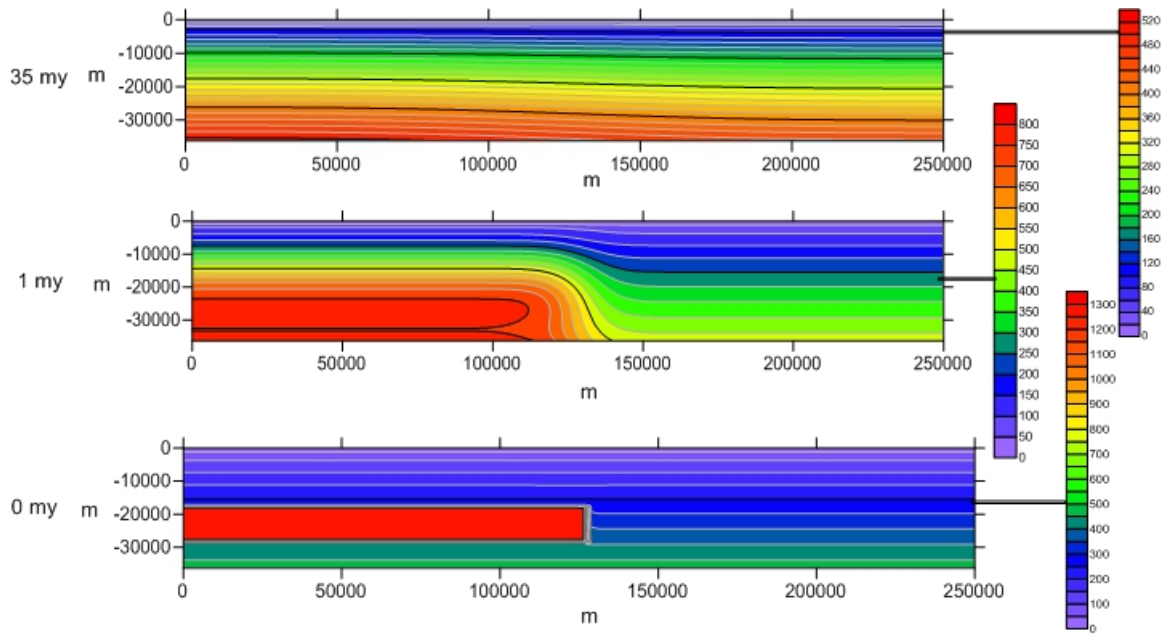


Figure 16. Results of heat flow simulation model run for 35 my duration. A 3650 km deep x 400 km wide section representing a slice through the Williston Basin was modeled.

In order to better visualize the crustal heating event that was simulated in the two model systems reported, a plot was generated in order to mathematically demonstrate the evolution of the temperature over time.

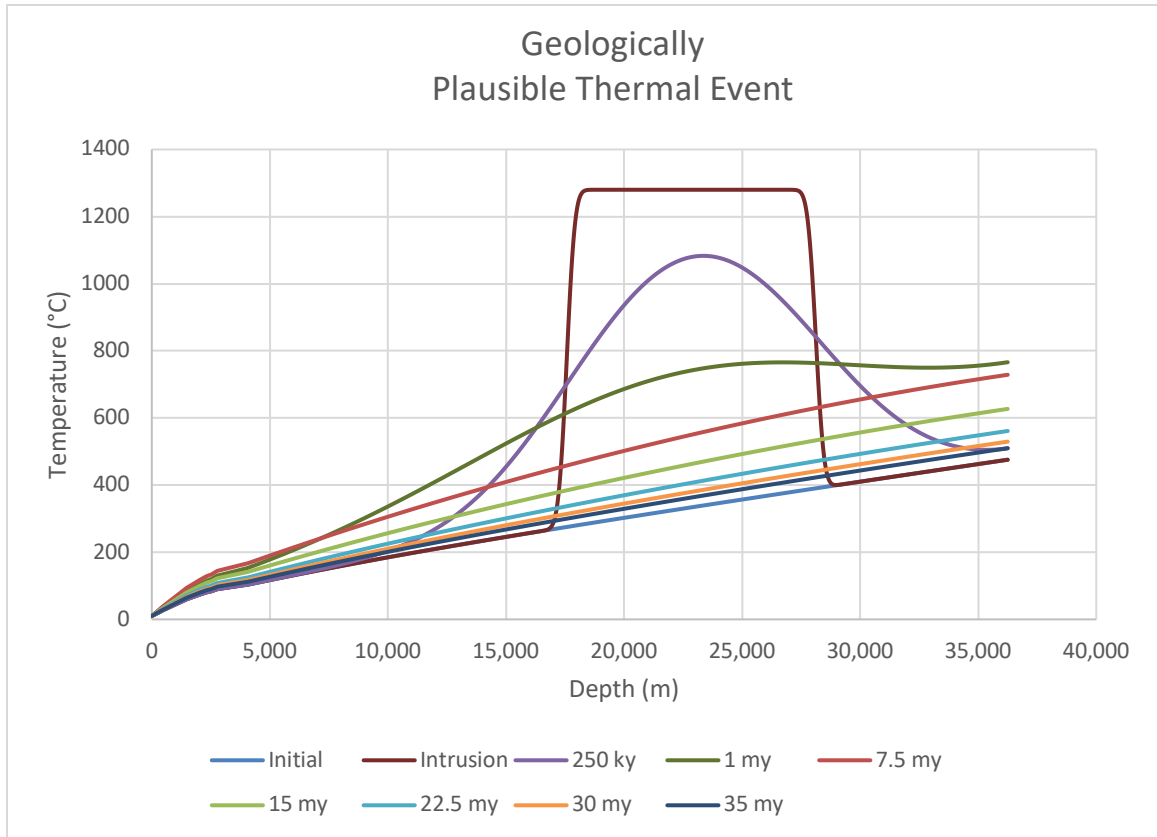


Figure 17. Plot of simulated thermal event evolution taking place in heat flow models.

Two plots were also generated in order to better demonstrate any difference that exists between the results of the two thermal event simulations spanning 35my and 65 my. Specifically, these plots demonstrate the evolution of surface heat flow,  $q$ , over time.

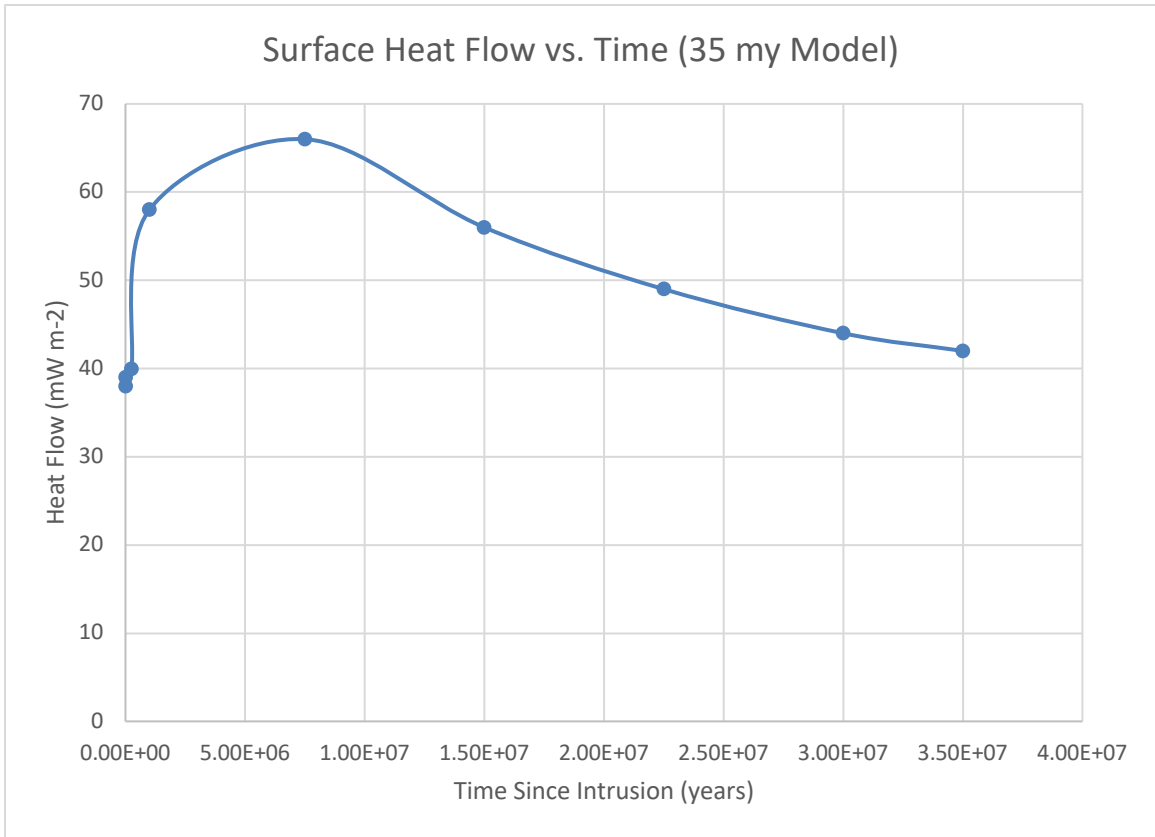


Figure 18. Plot of surface heat flow change over geologic time in the 35 my heat flow model.

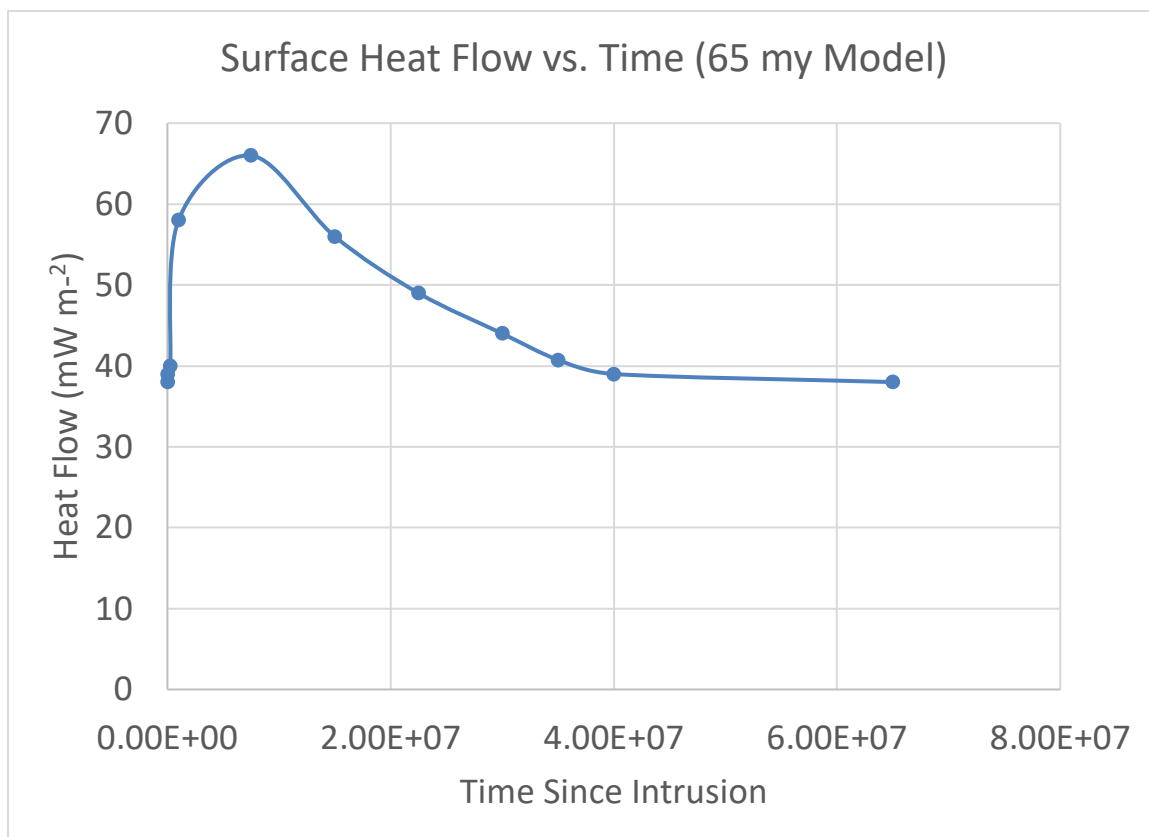


Figure 19. Plot of surface heat flow change over geologic time in the 65 my heat flow model.

After updating the heat flow simulation models to account for variability in the thermal regime heat flow, it is clear that the thermal pulse event could have occurred before the Eocene Epoch and still resulted in present day conditions within the Williston Basin. The thermal event demonstrated here would have caused significant uplift, accompanied by faulting and erosion. It may also exhibit high heat flow, depending on exactly when the geologic process was initiated. The Rio Grande, which did experience a thermal event beginning in the late Eocene Epoch, presents all of those characteristics today, in addition to standing an average of 2 km above sea level and containing some elevation offset in the northern portion as high as 5 km. In contrast, the Williston Basin, the surface of which lies within 500 m of sea level, was rapidly subsiding from the Early

Cretaceous through the Tertiary times and accumulated approximately 700 m of sediments from the Eocene through the Tertiary. There was no uplift, faulting, and erosion of the magnitude necessary, and there is no remnant thermal signal that might exist from whole crustal heating. As such, other geologic processes may account for the variable heat flow throughout the Basin.

## **CHAPTER IV**

### **DISCUSSION**

#### **Thermostратigraphy**

A significant amount of TSTRAT data has been collected for the North Dakota section of the Williston Basin to date. However, despite the amount of data that has been generated thus far, there still exists areas of the North Dakota map for which we have very little to no information concerning temperature and heat flow. It would be highly desirable for researchers to continue collecting such data for any existing wells not yet studied as well as new wells that are entered into the NDGS database. A systematic study of thermal conductivity measurements of rock samples stored in the Wilson Laird Core and Sample Library, temperature logs for wells located throughout the Williston Basin, and thermal modeling analysis with high precision and detail of several possible scenarios for basin evolution would be important aspects of such an investigation. By generating these datasets, it may be possible for the State of North Dakota to begin filling the gaps in knowledge of regional heat flow and maps created, such as those in McDonald (2015), that display such data. As the Williston Basin is one of the simpler sedimentary basin systems found anywhere in the world, the ramifications of having extensive temperature, heat flow, kinetics, and thermal maturation datasets on such an area, and the resulting insights that might be made from such study, would surely be of value to the global community and a major step forward for North Dakota. The effective



extent of drilling operations in the Williston Basin, known in the industry as the “magic line,” likely results not from any major structural constraining feature but, instead, from the extent of temperature and heat flow conditions. The results of these combined studies could possibly provide answers to many important temperature, heat flow, and thermal maturation questions raised but not yet satisfied.

Collecting vitrinite reflectance data for the shallow upper crust coals of the region may also help in constraint of the model system developed in this study. Since the maturation of vitrinite particles in sedimentary rocks is a kinetic process, the study of values obtained in such experiments can be useful in determinations involving temperature. Also, as so little data exists about the sediments above the Pierre Formation Shale, obtaining %R<sub>o</sub> measurements at these depths could be helpful to make determinations about previously speculated erosion amounts at those depths.

The Time-Temperature Index (TTI) approach, based on the Lopatin (1970) method, may provide another valuable dataset to help constrain the temperature models. The temperature history of source rock influences the chemical reactions that generate oil and gas. The TTI used by Nordeng (2008) helped determine the oil generation capacity of source rock for a particular interval under given time-temperature limits. However, the method might be reworked in order to provide the information sought in this study.

### **Steady State Heat Flow Conduction Modeling**

One useful exercise to add more data for study on the present topic would be to create acutely detailed models with respect to thicknesses and thermal conductivity values within the Basin in order to provide the foundation to incorporate previously suggested erosion amounts that are speculated to have occurred at each well. Price

(1996) developed a set of values that were determined from vitrinite reflectance data, and those values could be used to construct stratigraphic columns for each wellsite that could be modeled under the same conditions imposed in this study. As the elevated heat flow phenomenon of the Williston Basin is suspected to be basin-wide, the same elevated condition could be imposed on each wellsite model. Temperature conditions present in the resulting heat flow models could, then, be extrapolated and compared with the results of thermostratigraphy projections of temperature at depth in order to cross-validate datasets and present a compelling argument on the topic.

## **CHAPTER VI**

### **CONCLUSIONS**

Thermostратigraphy and updated simulation model data indicates that elevated heat flow may have existed in the Williston Basin at some time in the geologic past. However, there is no present or existing evidence that elevated heat flow in the Williston Basin was the result of rifting and uplifting in the Eocene Epoch or younger time frame. The data generated also indicates that the time frame necessary for an event that could have elevated the thermal regime of the Williston Basin and subsequently dissipated to allow for basin cooling could be much older than the Eocene Epoch. Only more dedicated and detailed study of numerous lines of geologic and geophysical evidence will allow for a rigorous explanation of the processes involved in these elevated heat flow conditions once existing throughout the Basin. As the Williston Basin is one of the simpler sedimentary basin systems found anywhere in the world, the ramifications of having extensive temperature, heat flow, kinetics, and thermal maturation datasets on such an area, and the resulting insights that might be made from such study, would surely be of value to the global research community and a major step forward for North Dakota.

## **APPENDICES**

## Appendix A

### Thermostратigraphy Datasets

Table 2. TSTRAT calculations for NDGS #25. Heat flow used for calculations is 62 mW m<sup>-2</sup> (McDonald, 2015).

NDGS #25			
Age	Formation	Temperature (°C)	Depth (m)
Tertiary	Brule Fm	10	16.5133387
Tertiary	Chadron Fm	10.60142843	28.15388893
Tertiary	Golden Valley Fm	12.64908243	61.18056633
Tertiary	Tongue R. Fm	18.69134013	168.3819126
Tertiary	Slope Fm.	19.9425147	190.5801712
Tertiary	Cannonball Fm.	21.13265637	211.6955879
Tertiary	Ludlow Fm	22.52115498	236.3302407
Cretaceous	Hell Creek Fm	24.06223586	263.6719982
Cretaceous	Fox hills Fm	25.9237395	296.6986756
Cretaceous	Pierre Fm	34.37407708	460.2535967
Cretaceous	Niobrara Fm	46.98126715	683.9295494
Cretaceous	Carlille Fm	64.1056083	1042.988316
Cretaceous	Greenhorn Fm	71.100387	1178.371129
Cretaceous	Belle fourche Fm	73.96838718	1233.88081
Cretaceous	Mowry Fm	76.40752753	1281.089978
Cretaceous	Newcastle Fm	78.502037	1321.628871
Cretaceous	Skull Creek Fm	79.0870497	1333.895266
Cretaceous	Inyan Kara Fm	81.90213988	1388.380883
Jurassic	Swift Fm	87.08723193	1522.18971
Jurassic	Rierdon Fm	93.73296874	1650.816874
Jurassic	Piper Fm	96.97720868	1734.539195
Triassic/Permian	Spearfish Fm	100.8668995	1834.918313
Permian	Minnekahta Fm	105.3905675	1951.658132
Permian	Opeche Fm	105.4661588	1954.706169
Permian	Broom Creek Fm	108.000057	2003.74936
Pennsylvanian	Amsden Fm	109.6610333	2062.68723
Pennsylvanian	Tyler Fm	110.2078219	2097.963911
Mississippian	Otter Fm	111.8666314	2170.20239
Mississippian	Kibbey Fm	114.4843308	2284.198976
Mississippian	Charles Fm	115.5482086	2330.529139
Mississippian	Mission Canyon Fm	125.3812848	2725.438164
Mississippian	Lodgepole Fm	130.3961536	2926.841767
Mississippian/Devonian	Bakken Fm	132.0022227	2991.343575
Devonian	Three Forks Fm	133.7373871	3022.128749
Devonian	Bird Bear Fm	136.5720615	3081.565472
Devonian	Duperow Fm	137.1033743	3108.388198
Devonian	Souris R. Fm	139.7040474	3242.197025
Devonian	Dawson Bay Fm	141.4061465	3322.3604
Devonian	Prairie Fm	142.3269862	3363.204097
Devonian	Winnepegosis Fm	143.6214875	3446.720312
Silurian	Interlake Fm	145.4859891	3536.637406

Table 3. TSTRAT calculations for NDGS #527. Heat flow used for calculations is 56 mW m<sup>-2</sup> (McDonald, 2015).

NDGS #527			
Age	Formation	Temperature (°C)	Depth (m)
Tertiary	Brule Fm	10	16.5133387
Tertiary	Chadron Fm	10.54322568	28.15388893
Tertiary	Golden Valley Fm	12.39271961	61.18056633
Tertiary	Tongue R. Fm	17.8502427	168.3819126
Tertiary	Slope Fm.	18.98033586	190.5801712
Tertiary	Cannonball Fm.	20.05530253	211.6955879
Tertiary	Ludlow Fm	21.30943031	236.3302407
Cretaceous	Hell Creek Fm	22.70137433	263.6719982
Cretaceous	Fox hills Fm	24.38273245	296.6986756
Cretaceous	Pierre Fm	41.46014628	662.6432577
Cretaceous	Niobrara Fm	54.17159647	912.3324579
Cretaceous	Carlille Fm	71.43755412	1313.149332
Cretaceous	Greenhorn Fm	78.49017889	1464.277006
Cretaceous	Belle fourche Fm	81.88774473	1537.081988
Cretaceous	Mowry Fm	84.77726334	1599.000244
Cretaceous	Newcastle Fm	85.63955303	1617.47788
Cretaceous	Skull Creek Fm	86.38360232	1634.750453
Cretaceous	Inyan Kara Fm	89.96397906	1711.472812
Jurassic	Swift Fm	93.6018113	1815.410875
Jurassic	Rierdon Fm	102.2358843	2000.426725
Jurassic	Piper Fm	104.8217119	2074.307515
Triassic/Permian	Spearfish Fm	107.9219974	2162.887101
Permian	Minnekahta Fm	112.3599394	2289.685443
Permian	Opeche Fm	112.6398711	2302.182395
Permian	Broom Creek Fm	117.0778131	2397.281151
Pennsylvanian	Amsden Fm	118.4902044	2452.767952
Pennsylvanian	Tyler Fm	118.9551595	2485.97903
Mississippian	Otter Fm	120.7735464	2573.651255
Mississippian	Kibbey Fm	123.0390776	2682.882224
Mississippian	Charles Fm	123.9114935	2724.945135
Mississippian	Mission Canyon Fm	130.2898428	3008.553882
Mississippian	Lodgepole Fm	133.542801	3153.194343
Mississippian/Devonian	Bakken Fm	139.3764257	3412.582297
Devonian	Three Forks Fm	140.8040154	3440.624238
Devonian	Bird Bear Fm	143.9552168	3513.777128
Devonian	Duperow Fm	144.4569256	3541.819069

Table 4. TSTRAT calculations for NDGS #607. Heat flow used for calculations is 52 mW m<sup>-2</sup> (McDonald, 2015).

NDGS #607			
Age	Formation	Temperature (°C)	Depth (m)
Tertiary	Brule Fm	10	16.5133387
Tertiary	Chadron Fm	10.50442384	28.15388893
Tertiary	Golden Valley Fm	12.22181107	61.18056633
Tertiary	Tongue R. Fm	17.28951108	168.3819126
Tertiary	Slope Fm.	18.3388833	190.5801712
Tertiary	Cannonball Fm.	19.33706663	211.6955879
Tertiary	Ludlow Fm	20.50161386	236.3302407
Cretaceous	Hell Creek Fm	21.7941333	263.6719982
Cretaceous	Fox hills Fm	23.35539442	296.6986756
Cretaceous	Pierre Fm	34.35238987	550.4754938
Cretaceous	Niobrara Fm	46.15587933	800.1646939
Cretaceous	Carlille Fm	62.18855429	1200.981568
Cretaceous	Greenhorn Fm	66.51844917	1300.902219
Cretaceous	Belle fourche Fm	69.67333174	1373.707201
Cretaceous	Mowry Fm	72.30362352	1434.406242
Cretaceous	Newcastle Fm	73.10432108	1452.883878
Cretaceous	Skull Creek Fm	73.795224	1470.156451
Cretaceous	Inyan Kara Fm	76.72361472	1537.734699
Jurassic	Swift Fm	80.56718946	1655.998537
Jurassic	Rierdon Fm	86.69577598	1797.427457
Jurassic	Piper Fm	89.09690165	1871.308247
Triassic/Permian	Spearfish Fm	92.10451775	1963.85028
Permian	Minnekahta Fm	94.74945192	2045.23287
Permian	Opeche Fm	95.0030486	2057.425018
Permian	Broom Creek Fm	101.2373004	2201.292368
Pennsylvanian	Amsden Fm	102.5488066	2256.779168
Pennsylvanian	Tyler Fm	103.6581293	2342.11168
Mississippian	Otter Fm	104.6149871	2391.794684
Mississippian	Kibbey Fm	106.4817405	2488.722263
Mississippian	Charles Fm	107.6616695	2549.987808
Mississippian	Mission Canyon Fm	115.8098613	2940.160839
Mississippian	Lodgepole Fm	119.9654391	3139.149085
Mississippian/Devonian	Bakken Fm	121.2963105	3202.877347
Devonian	Three Forks Fm	122.6219295	3230.919288
Devonian	Bird Bear Fm	125.621198	3305.901
Devonian	Duperow Fm	126.1478365	3337.600585

Table 5. TSTRAT calculations for NDGS #2010. Heat flow used for calculations is 48 mW m<sup>-2</sup> (McDonald, 2015).

NDGS #2010			
Age	Formation	Temperature (°C)	Depth (m)
Tertiary	Brule Fm	10	16.5133387
Tertiary	Chadron Fm	10.46562201	28.15388893
Tertiary	Golden Valley Fm	12.05090252	61.18056633
Tertiary	Tongue R. Fm	16.72877945	168.3819126
Tertiary	Slope Fm.	17.69743074	190.5801712
Tertiary	Cannonball Fm.	18.61883074	211.6955879
Tertiary	Ludlow Fm	19.69379741	236.3302407
Cretaceous	Hell Creek Fm	20.88689228	263.6719982
Cretaceous	Fox hills Fm	22.32805639	296.6986756
Cretaceous	Pierre Fm	21.79880724	283.467447
Cretaceous	Niobrara Fm	32.69433597	533.1566471
Cretaceous	Carlille Fm	47.49372824	933.9735211
Cretaceous	Greenhorn Fm	52.85607489	1068.032187
Cretaceous	Belle fourche Fm	54.3780614	1106.08185
Cretaceous	Mowry Fm	55.67246114	1138.441843
Cretaceous	Newcastle Fm	57.73293419	1189.95367
Cretaceous	Skull Creek Fm	58.29132015	1205.076623
Cretaceous	Inyan Kara Fm	60.97828206	1272.250671
Jurassic	Swift Fm	63.45633619	1354.852475
Jurassic	Rierdon Fm	70.34489996	1527.066569
Jurassic	Piper Fm	72.9106287	1612.590861
Triassic/Permian	Spearfish Fm	75.98681656	1715.130456
Permian	Minnekahta Fm	76.06826994	1717.845569
Permian	Opeche Fm	76.44559301	1737.497812
Permian	Broom Creek Fm	77.0351603	1752.236994
Pennsylvanian	Amsden Fm	77.42162308	1769.949871
Pennsylvanian	Tyler Fm	77.54884549	1780.551739
Mississippian	Otter Fm	77.68905448	1788.438495
Mississippian	Kibbey Fm	77.86374109	1798.264616
Mississippian	Charles Fm	78.55329348	1837.051939
Mississippian	Mission Canyon Fm	84.5753357	2149.445379
Mississippian	Lodgepole Fm	87.64657723	2308.766033
Mississippian/Devonian	Bakken Fm	88.63017746	2359.790295
Devonian	Three Forks Fm	89.77402264	2386.003414
Devonian	Bird Bear Fm	91.6422349	2436.600829
Devonian	Duperow Fm	92.12368842	2467.995611
Devonian	Souris R. Fm	94.44898717	2622.53109
Devonian	Dawson Bay Fm	96.28281988	2734.089247
Devonian	Prairie Fm	96.9744472	2773.713728
Devonian	Winnepegosis Fm	98.1010017	2867.59327
Silurian	Interlake Fm	99.08452884	2928.858815
Silurian/Ordovician	Stonewall Fm	99.42852634	2955.876952
Ordovician	Stony Mountain Fm	100.1133187	3011.373666
Ordovician	Red River Fm	102.0831785	3166.91051
Ordovician	Winnipeg Fm	103.9922905	3297.366496



Table 6. TSTRAT calculations for NDGS #2615. Heat flow used for calculations is 54 mW m<sup>-2</sup> (McDonald, 2015).

NDGS #2615			
Age	Formation	Temperature (°C)	Depth (m)
Tertiary	Brule Fm	10	16.5133387
Tertiary	Chadron Fm	10.52382476	28.15388893
Tertiary	Golden Valley Fm	12.30726534	61.18056633
Tertiary	Tongue R. Fm	17.56987689	168.3819126
Tertiary	Slope Fm.	18.65960958	190.5801712
Tertiary	Cannonball Fm.	19.69618458	211.6955879
Tertiary	Ludlow Fm	20.90552208	236.3302407
Cretaceous	Hell Creek Fm	22.24775382	263.6719982
Cretaceous	Fox hills Fm	23.86906343	296.6986756
Cretaceous	Pierre Fm	48.2782302	839.1246038
Cretaceous	Niobrara Fm	60.33529272	1084.731433
Cretaceous	Carlille Fm	76.71239587	1478.995027
Cretaceous	Greenhorn Fm	83.4019503	1627.651792
Cretaceous	Belle fourche Fm	86.93760402	1706.221875
Cretaceous	Mowry Fm	89.94456185	1773.04316
Cretaceous	Newcastle Fm	90.77380211	1791.470721
Cretaceous	Skull Creek Fm	91.48933383	1808.696485
Cretaceous	Inyan Kara Fm	94.93248359	1885.210924
Jurassic	Swift Fm	98.7078585	1997.073884
Jurassic	Rierdon Fm	105.7031036	2152.523775
Jurassic	Piper Fm	107.9860615	2220.166974
Triassic/Permian	Spearfish Fm	110.7232206	2301.267983
Permian	Minnekahta Fm	114.9820904	2427.456718
Permian	Opeche Fm	115.2322733	2439.039259
Permian	Broom Creek Fm	120.554146	2557.303097
Pennsylvanian	Amsden Fm	123.0674328	2659.696265
Pennsylvanian	Tyler Fm	123.8947995	2720.982687
Mississippian	Otter Fm	125.1976685	2786.126136
Mississippian	Kibbey Fm	126.8209151	2867.288466
Mississippian	Charles Fm	127.6987498	2911.1802
Mississippian	Mission Canyon Fm	133.1707704	3163.501149
Mississippian	Lodgepole Fm	135.9615009	3292.184833
Mississippian/Devonian	Bakken Fm	141.7123756	3557.364058
Devonian	Three Forks Fm	142.7448289	3578.395513
Devonian	Bird Bear Fm	145.8974371	3654.291636
Devonian	Duperow Fm	146.3864864	3682.638381

Table 7. TSTRAT calculations for NDGS #6464. Heat flow used for calculations is 55 mW m<sup>-2</sup> (McDonald, 2015).

NDGS #6464			
Age	Formation	Temperature (°C)	Depth (m)
Tertiary	Brule Fm	10	16.5133387
Tertiary	Chadron Fm	10.53352522	28.15388893
Tertiary	Golden Valley Fm	12.34999248	61.18056633
Tertiary	Tongue R. Fm	17.71005979	168.3819126
Tertiary	Slope Fm.	18.81997272	190.5801712
Tertiary	Cannonball Fm.	19.87574355	211.6955879
Tertiary	Ludlow Fm	21.1074762	236.3302407
Cretaceous	Hell Creek Fm	22.47456407	263.6719982
Cretaceous	Fox hills Fm	24.12589794	296.6986756
Cretaceous	Pierre Fm	41.68068747	679.7122653
Cretaceous	Niobrara Fm	53.73792261	920.8569681
Cretaceous	Carlille Fm	70.11526022	1307.957675
Cretaceous	Greenhorn Fm	76.80491042	1453.91368
Cretaceous	Belle fourche Fm	80.39094013	1532.154328
Cretaceous	Mowry Fm	83.44074111	1598.69544
Cretaceous	Newcastle Fm	85.159072	1636.186296
Cretaceous	Skull Creek Fm	85.73490753	1649.796954
Cretaceous	Inyan Kara Fm	88.50583699	1710.253597
Jurassic	Swift Fm	92.63402219	1830.346257
Jurassic	Rierdon Fm	99.68895798	1984.272129
Jurassic	Piper Fm	102.1428433	2055.657883
Triassic/Permian	Spearfish Fm	105.0849361	2141.246038
Permian	Minnekahta Fm	109.2759871	2263.16752
Permian	Opeche Fm	109.55092	2275.664472
Permian	Broom Creek Fm	114.4963601	2383.564984
Pennsylvanian	Amsden Fm	117.022821	2484.623419
Pennsylvanian	Tyler Fm	117.8545245	2545.110949
Mississippian	Otter Fm	118.4940479	2576.50573
Mississippian	Kibbey Fm	120.6485585	2682.272616
Mississippian	Charles Fm	121.5799032	2727.993172
Mississippian	Mission Canyon Fm	127.8443534	3011.601919
Mississippian	Lodgepole Fm	130.1976465	3118.141917
Mississippian/Devonian	Bakken Fm	136.0280885	3382.101926
Devonian	Three Forks Fm	137.1253818	3404.047793
Devonian	Bird Bear Fm	140.0526697	3473.238235
Devonian	Duperow Fm	140.4972157	3498.536942
Devonian	Souris R. Fm	142.4206322	3610.095099
Devonian	Dawson Bay Fm	143.9248176	3689.95367
Devonian	Prairie Fm	144.6502504	3726.225311
Devonian	Winnepegosis Fm	145.1447945	3762.192148
Silurian	Interlake Fm	146.8436419	3854.547671
Silurian/Ordovician	Stonewall Fm	147.5285078	3901.492117
Ordovician	Stony Mountain Fm	148.8918635	3997.918546
Ordovician	Red River Fm	152.8136647	4268.166301

Table 8. TSTRAT calculations for NDGS #6616. Heat flow used for calculations is 50 mW m<sup>-2</sup> (McDonald, 2015).

NDGS #6616			
Age	Formation	Temperature (°C)	Depth (m)
Tertiary	Brule Fm	10	41.04859165
Tertiary	Chadron Fm	11.20566219	69.98448413
Tertiary	Golden Valley Fm	15.31052135	152.0816674
Tertiary	Tongue R. Fm	27.42322053	418.5610493
Tertiary	Slope Fm.	29.93140571	473.7411234
Tertiary	Cannonball Fm.	32.3172404	526.2294865
Tertiary	Ludlow Fm	35.1007142	587.4659101
Cretaceous	Hell Creek Fm	38.19006424	655.431611
Cretaceous	Fox hills Fm	41.92175439	737.5287943
Cretaceous	Pierre Fm	61.5768519	1209.251134
Cretaceous	Niobrara Fm	63.90151134	1260.393642
Cretaceous	Carlille Fm	67.05909531	1342.490825
Cretaceous	Greenhorn Fm	68.34887346	1373.445501
Cretaceous	Belle fourche Fm	71.08729616	1439.167646
Cretaceous	Mowry Fm	73.41623508	1495.06218
Cretaceous	Newcastle Fm	75.38475902	1542.306754
Cretaceous	Skull Creek Fm	75.85438919	1554.517139
Cretaceous	Inyan Kara Fm	78.11425684	1608.753962
Jurassic	Swift Fm	83.15304311	1769.995123
Jurassic	Rierdon Fm	89.16021616	1914.167276
Jurassic	Piper Fm	91.73322209	1996.503466
Triassic/Permian	Spearfish Fm	94.81813496	2095.220678
Permian	Minnekahta Fm	98.55198036	2214.703731
Permian	Opeche Fm	98.73486259	2223.847842
Permian	Broom Creek Fm	101.7352335	2295.856745
Pennsylvanian	Amsden Fm	103.7019839	2382.39376
Pennsylvanian	Tyler Fm	104.3494323	2434.189637
Mississippian	Otter Fm	105.0629709	2472.720717
Mississippian	Kibbey Fm	105.9519697	2520.726652
Mississippian	Charles Fm	106.759135	2564.313582
Mississippian	Mission Canyon Fm	112.7621443	2863.263442
Mississippian	Lodgepole Fm	115.823679	3015.727871
Mississippian/Devonian	Bakken Fm	120.169274	3232.138503
Devonian	Three Forks Fm	120.9867021	3250.121921
Devonian	Bird Bear Fm	123.3899621	3312.606681
Devonian	Duperow Fm	123.8379164	3340.648622
Devonian	Souris R. Fm	125.9591209	3475.981468
Devonian	Dawson Bay Fm	127.2169581	3549.439161
Devonian	Prairie Fm	127.8764425	3585.710802
Devonian	Winnepegosis Fm	128.5660609	3640.880273
Silurian	Interlake Fm	130.0544001	3729.882955
Silurian/Ordovician	Stonewall Fm	130.5467034	3767.002624
Ordovician	Stony Mountain Fm	131.5267266	3843.24843
Ordovician	Red River Fm	134.3458414	4056.937332
Ordovician	Winnipeg Fm	132.2389778	3918.727081
Ordovician	Erosion	133.7744986	4043.718477
Ordovician	Deadwood Fm	133.7744986	4043.718477

Table 9. TSTRAT calculations for NDGS #7020. Heat flow used for calculations is 48 mW m<sup>-2</sup> (McDonald, 2015).

NDGS #7020			
Age	Formation	Temperature (°C)	Depth (m)
Tertiary	Brule Fm	10	31.93882875
Tertiary	Chadron Fm	10.90057025	54.45308508
Tertiary	Golden Valley Fm	13.96669781	118.3307426
Tertiary	Tongue R. Fm	23.01428733	325.6713358
Tertiary	Slope Fm.	24.88777809	368.605499
Tertiary	Cannonball Fm.	26.66987906	409.4453128
Tertiary	Ludlow Fm	28.74899685	457.0917623
Cretaceous	Hell Creek Fm	31.05658913	509.9740853
Cretaceous	Fox hills Fm	33.84397782	573.8517428
Cretaceous	Pierre Fm	48.5253673	940.8864797
Cretaceous	Niobrara Fm	50.26177337	980.6791188
Cretaceous	Carlille Fm	52.62033303	1044.556776
Cretaceous	Greenhorn Fm	53.58373377	1068.641795
Cretaceous	Belle fourche Fm	56.2389743	1135.022808
Cretaceous	Mowry Fm	58.49716951	1191.477688
Cretaceous	Newcastle Fm	59.78953723	1223.786881
Cretaceous	Skull Creek Fm	60.29622079	1237.509561
Cretaceous	Inyan Kara Fm	62.73438992	1298.463789
Jurassic	Swift Fm	65.53248795	1391.733723
Jurassic	Rierdon Fm	70.61661377	1518.836869
Jurassic	Piper Fm	72.07205147	1567.351459
Triassic/Permian	Spearfish Fm	73.81705269	1625.518166
Permian	Minnekahta Fm	74.30169058	1641.672763
Permian	Opeche Fm	74.54748429	1654.474518
Permian	Broom Creek Fm	76.08369497	1692.879785
Pennsylvanian	Amsden Fm	77.77274022	1770.29436
Pennsylvanian	Tyler Fm	78.32876899	1816.63009
Mississippian	Otter Fm	79.2552536	1868.744849
Mississippian	Kibbey Fm	80.40956229	1933.674713
Mississippian	Charles Fm	81.0760664	1971.165569
Mississippian	Mission Canyon Fm	84.18514689	2132.44912
Mississippian	Lodgepole Fm	85.77077794	2214.703731
Mississippian/Devonian	Bakken Fm	87.2784644	2292.914966
Devonian	Three Forks Fm	92.98977091	2423.799073
Devonian	Bird Bear Fm	95.11683186	2481.406974
Devonian	Duperow Fm	95.43468467	2502.133626
Devonian	Souris R. Fm	96.64549112	2582.601804
Devonian	Dawson Bay Fm	96.78464962	2591.06728
Devonian	Prairie Fm	97.28907522	2619.966664
Devonian	Winnepegosis Fm	97.53778507	2640.692484
Silurian	Interlake Fm	98.32272829	2689.587905
Silurian/Ordovician	Stonewall Fm	98.62708459	2713.492557
Ordovician	Stony Mountain Fm	99.23296362	2762.594003
Ordovician	Red River Fm	100.9758229	2900.207267
Ordovician	Winnipeg Fm	103.9197806	3101.377713
Ordovician	Erosion	104.4661806	3147.707876
Ordovician	Deadwood Fm	107.1122251	3340.648622

Table 10. TSTRAT calculations for NDGS #7783. Heat flow used for calculations is 40 mW m<sup>-2</sup> (McDonald, 2015).

NDGS #7783			
Age	Formation	Temperature (°C)	Depth (m)
Tertiary	Brule Fm	10	38.78026069
Tertiary	Chadron Fm	10.91123017	66.11716577
Tertiary	Golden Valley Fm	14.01365102	143.6776872
Tertiary	Tongue R. Fm	23.16833552	395.4315107
Tertiary	Slope Fm.	25.06400251	447.5623529
Tertiary	Cannonball Fm.	26.86719794	497.1502272
Tertiary	Ludlow Fm	28.97092594	555.0027473
Cretaceous	Hell Creek Fm	31.30583284	619.2126871
Cretaceous	Fox hills Fm	34.12621544	696.7732085
Cretaceous	Pierre Fm	48.98138634	1142.428335
Cretaceous	Niobrara Fm	50.73834598	1190.744726
Cretaceous	Carlille Fm	53.12482357	1268.305247
Cretaceous	Greenhorn Fm	54.09962793	1297.549378
Cretaceous	Belle fourche Fm	56.22447923	1361.294917
Cretaceous	Mowry Fm	58.03159575	1415.508413
Cretaceous	Newcastle Fm	58.58241959	1432.033128
Cretaceous	Skull Creek Fm	59.0577124	1447.480144
Cretaceous	Inyan Kara Fm	61.34482878	1516.093636
Jurassic	Swift Fm	64.28618455	1633.747866
Jurassic	Rierdon Fm	68.69567817	1766.032675
Jurassic	Piper Fm	70.47339136	1837.141202
Triassic/Permian	Spearfish Fm	72.6047857	1922.396976
Permian	Minnekahta Fm	72.81753164	1930.906814
Permian	Opeche Fm	73.80305188	1992.501829
Permian	Broom Creek Fm	74.76826362	2021.458181
Pennsylvanian	Amsden Fm	76.21740343	2101.160871
Pennsylvanian	Tyler Fm	76.69445603	2148.86613
Mississippian	Otter Fm	77.49065374	2202.609476
Mississippian	Kibbey Fm	78.48263777	2269.568398
Mississippian	Charles Fm	79.12385446	2312.850524
Mississippian	Mission Canyon Fm	82.97291427	2552.454497
Mississippian	Lodgepole Fm	84.93593477	2674.652524
Mississippian/Devonian	Bakken Fm	88.7943335	2914.837844
Devonian	Three Forks Fm	89.60344879	2937.088515
Devonian	Bird Bear Fm	91.64797827	3003.535723
Devonian	Duperow Fm	92.03750377	3034.016094
Devonian	Souris R. Fm	93.58923173	3157.766398
Devonian	Dawson Bay Fm	94.62472925	3233.357718
Devonian	Prairie Fm	95.31635657	3280.907096
Devonian	Winnepegosis Fm	95.87109932	3336.38137
Silurian	Interlake Fm	97.31458443	3444.281882
Silurian/Ordovician	Stonewall Fm	97.78183669	3488.320408
Ordovician	Stony Mountain Fm	98.71199106	3578.77792
Ordovician	Red River Fm	101.3876542	3832.297001
Ordovician	Winnipeg Fm	103.926446	4040.477932
Ordovician	Erosion	104.8910337	4138.624726

## Appendix B

### Heat Flow Profile Datasets

Table 11. Surface heat flow profile calculations for 35 my heat flow model.

Age (years)	HF (mW m <sup>-2</sup> )
0	38
1000	39
250000	40
1.00E+06	58
7.50E+06	66
1.50E+07	56
2.25E+07	49
3.00E+07	44
3.50E+07	42

Table 12. Surface heat flow profile calculations for 65 my heat flow model.

Age (years)	HF (mW m <sup>-2</sup> )
0	38
1000	39
250000	40
1.00E+06	58
7.50E+06	66
1.50E+07	56
2.25E+07	49
3.00E+07	44
3.50E+07	42
4.00E+07	39
6.50E+07	38

## REFERENCES

- Beardsmore, G.R. and Cull, J.P. (2001), *Crustal Heat Flow, A Guide to Measurement and Modelling*. Cambridge University Press.
- Blackwell, D.D. (1971), The Thermal Structure of the Continental Crust, in *The Structure and Physical Properties of the Earth's Crust*, Geophysical Monograph 14, edited by J.G. Heacock, p. 169 - 184.
- Brott, C.A., Blackwell, D.D., and Mitchell, J.C., (1978), Tectonic Implications of the Heat Flow of the western Snake River Plain, Idaho: *Geological Society of America Bulletin*, v. 89, p. 1697-1707.
- Burrus, J., K. Osadetz, S. Wolf, B. Doligez, and K. Visser (1995), Resolution of Williston Basin Oil System Paradoxes Through Basin Modelling, *Seventh International Williston Basin Symposium*, pp. 235–251, Saskatchewan.
- Burrus, J., K. Osadetz, S. Wolf, B. Doligez, K. Visser, and D. Dearborn (1996), A Two-Dimensional Regional Basin Model of Williston Basin Hydrocarbon Systems, *Am Assoc Pet Geol Bull*, 80(2), 265–290, doi:10.1306/64ED87AA-1724-11D7-8645000102C1865D.
- Cengel, Y., and A. Ghajar (2015), *Heat and Mass Transfer: Fundamentals and Applications*, 5 ed., McGraw-Hill.
- Clauser, C. (2009), Heat Transport Processes in the Earth's Crust, *Surv Geophys*, 30(3), 163–191, doi:10.1007/s10712-009-9058-2.
- Combs, J. and G. Simmons (1973), Terrestrial Heat Flow Determinations in the North Central United States, *Journal of Geophysical Research*, 78(2), 441-461.
- Crough, S. T. and G. A. Thompson (1976), Thermal Model of Continental Lithosphere, *Journal of Geophysical Research*, vol. 81, no. 26, p. 4857 - 4862.
- Crowell, A. M. (2011), Identifying Potential Geothermal Resources from Co-Produced Fluids Using Existing Data from Drilling Logs: Williston Basin, North Dakota, 1–51 pp. Grand Forks, ND, April.

- Crowell, J. (2015), Improving the Availability of Thermal Conductivity Data and Modeling How Inaccurate Thermal Conductivity Data Affect Geothermal Power Production Models, 1–80 pp. University of North Dakota, Grand Forks, ND.
- Gerhard, L. C., S. B. Anderson, J. A. LeFever, and C. G. Carlson (1982), Geological Development, Origin, and Energy and Mineral Resources of Williston Basin, North Dakota, *Am Assoc Pet Geol Bull*, 66(8), 989–1020, doi:10.1306/03B59D78-16D1-11D7-8645000102C1865D.
- Golden Software Inc., (2013). Surfer Version 11.4.958, Golden, CO.
- Gosnold, W. D., Jr (1984), Geothermal Resources in the Williston Basin: North Dakota, *GRC Trans*, vol. 8, pp. 431–436, Davis, CA.
- Gosnold, W. D., Jr, and Y. C. Huang (1987), Factors Determining the Thermal History of a Continental Basin, Fifth International Williston Basin Symposium, pp. 17–21, Saskatchewan.
- Gosnold, W. D. (1990), Heat Flow in the Great Plains of the United States, *J Geophys Res*, 95(B1), 353, doi:10.1029/jb095ib01p00353.
- Gosnold, W. D., Jr (1991), Subsurface Temperatures in the Northern Great Plains, in *Neotectonics of North America*, edited by D. B. Slemmons, pp. 467–472, Geological Society of America, Denver, CO.
- Gosnold, W. D., Jr (1999), Stratabound Geothermal Resources in North Dakota and South Dakota, *Nat Resour Res*, 8(3), 177–192, doi:10.1023/A:1021689813375.
- Gosnold, W. D., J. A. Majorowicz, R. Klenner, and S. A. Hauck (2010), Implications of Post-Glacial Warming for Northern Hemisphere Heat Flow, vol. 35.
- Gosnold, W. D., M. R. McDonald, R. Klenner, and D. Merriam (2012), *Thermostrostratigraphy of the Williston Basin*, vol. 36, pp. 663–670.
- Gosnold, W. D., Apostal, D., (2017), Finite Difference Heat Flow Simulation Version 2.5.4, Grand Forks, ND.
- Heck T.J., LeFever, R.D., Fischer, D.W., and J. LeFever, (2010). Overview of the Petroleum Geology of the North Dakota Williston Basin. <<https://www.dmr.nd.gov/ndgs/Resources/> > Accessed 8/16, 2017.
- HIS Inc., (2013). PETRA Version 3.8.3, Tulsa, OK.
- Lachenbruch, A. H. (1968), Preliminary Geothermal Model of the Sierra Nevada, *J Geophys Res*, 73(2), 6977–6989, doi:10.1029/JB073i022p06977.



- Lachenbruch, A. H. (1970), Crustal Temperature and Heat Production: Implications of the Linear Heat-Flow Relation, *J Geophys Res*, 75(17), 3291–3300, doi:10.1029/JB075i017p03291.
- Lund, J. W., L. Bjelm, G. Bloomquist, and A. K. Mortensen (2008), Characteristics, Development and Utilization of Geothermal Resources-a Nordic Perspective, *Episodes*, 140–147.
- Majorowicz, J. A., F. W. Jones, and A. M. Jessop (1986), Geothermics of the Williston Basin in Canada in Relation to Hydrodynamics and Hydrocarbon Occurrences, *Geophysics*, 51(3), 767–779, doi:10.1190/1.1442129.
- Majorowicz, J. A., F. W. Jones, and K. G. Osadetz (1988), Heat Flow Environment of the Electrical Conductivity Anomalies in the Williston Basin, and Occurrence of Hydrocarbons, *Bull Can Pet Geol*, 36(1), 86–90.
- McDonald, M. R. (2015), Preliminary Results of Temperature Logging in the Williston Basin to Determine Heat Flow, edited by E. C. Murphy and L. D. Helms, North Dakota Geological Survey, Grand Forks, ND.
- Morgan, P. (1984), The Thermal Structure and Thermal Evolution of the Continental Lithosphere, *Phys Chem Earth*, 15, 107–193, doi:10.1016/0079-1946(84)90006-5.
- Morgan, P., and W. D. Gosnold (1989), Heat Flow and Thermal Regimes in the Continental United States, in *Geophysical Framework of the Continental United States*, vol. 172, edited by L. C. Pakiser and W. D. Mooney, pp. 493–522, Geological Society of America, Boulder, CO.
- Murphy, E. C., S. H. Nordeng, B. J. Juenker, and J. W. Hoganson (2009), North Dakota Stratigraphic Column, edited by E. C. Murphy and L. D. Helms, North Dakota Geological Survey, Grand Forks, ND.
- Pollack, H. N., (1982), The Heat Flow from the Continents. *Annual Review of Earth and Planetary Sciences*, vol. 10, p. 459 - 481.
- Porter, J. W., R. A. Price, and R. G. McCrossan (1982), The Western Canada Sedimentary Basin, *Philosophical Transactions of the Royal Society A: Mathematical, Physical and Engineering Sciences*, 305(1489), 169–192, doi:10.1098/rsta.1982.0032.
- Price, L. C. (1996), Origins and Characteristics of the Basin-Centered Continuous-Reservoir Unconventional Oil-Resource Base of the Bakken Source System, Williston Basin, Unpublished, 1–281.
- Price, L. C., T. Ging, T. Daws, A. Love, M. Pawlewicz, and D. Anders (2011), Organic Metamorphism in the Mississippian-Devonian Bakken Shale North Dakota Portion of the

Williston Basin, in *The Bakken—Three Forks Petroleum System in the Williston Basin*, edited by J. W. Robinson, J. A. LeFever, and S. B. Gaswirth, pp. 438–489, The Rocky Mountain Association of Geologists.

Ricker, F. N. (2015), *Geothermal Regime of the Williston Basin in North Dakota*, The University of North Dakota, Grand Forks, ND.

Scatollini, R. (1978), *Heat-Flow and Heat-Production Studies in North Dakota*, 1–264 pp. The University of North Dakota, Grand Forks, ND.

Roy, R. F., D. D. Blackwell, and F. Birch (1968), Heat Generation of Plutonic Rocks and Continental Heat Flow Provinces, *Earth Planet Sci Lett*, 5, 1–12, doi:10.1016/S0012-821X(68)80002-0.

Roy, R. F., E. R. Decker, D. D. Blackwell, and F. Birch (1968), Heat Flow in the United States, *J Geophys Res*, 73(1), 5207–5221, doi:10.1029/JB073i016p05207.

Sclater, J. G., C. Jaupart, and D. Galson (1980), The Heat Flow Through Oceanic and Continental Crust and the Heat Loss of the Earth, *Rev Geophys*, 18(1), 269–311, doi:10.1029/RG018i001p00269.

Sloss L.L. (1963), Sequences in the Cratonic Interior of North America, *Geological Society of America Bulletin*, vol. 74, p. 93 - 114.